ABSTRACT OF THE THESIS OF

Robert Kenneth Lane (Name) for the Doctor of Philosophy (Degree) in Oceanography (Major)

Date thesis is presented: April 20, 1965

Title CLIMATE AND HEAT EXCHANGE IN THE OCEANIC REGION ADJACENT TO OREGON

Abstract approved: Redacted for privacy
(Major Professor)

The climate and the exchange of heat between atmosphere and ocean are examined in a region adjacent to Washington and Oregon, and in two sub-regions adjacent to Oregon. The sub-regions are chosen such that one contains the nearshore upwelling region and the other borders it on the seaward side.

The data (ship weather observations, 1953 to 1962) reveal the general seasonal variation of climatic factors in the regions studied and the effects of the nearshore upwelling of cold water on the climate over the coastal ocean region and the adjacent coastal land mass. In the nearshore sub-region, summer values of temperature (air, wet bulb, and sea surface) are lower than those to seaward, but winter values are higher inshore than to seaward. The effects of these differences, and of other factors, on the heat exchange processes are examined with the use of empirical equations. It is seen that the processes of evaporation and conduction are suppressed considerably

and net long wave radiation is slightly suppressed in the upwelling region during the summer.

The effects of the reduction of heat loss to the atmosphere in the summer upwelling region on the climate of coastal Oregon are seen to be a slight reduction of air temperatures and, despite reduced evaporation, a very slight increase of relative humidity.

Monthly means of daily net heat exchange between the sea and the atmosphere are examined and correlated with the difference between monthly means of the heat used per day in the oceanic evaporation process and the monthly means of daily totals of heat estimated to be used in the evaporation from a shallow pan under climatic conditions identical to those accompanying the net heat exchange and oceanic evaporation.

CLIMATE AND HEAT EXCHANGE IN THE OCEANIC REGION ADJACENT TO OREGON

by

ROBERT KENNETH LANE

A THESIS

submitted to

OREGON STATE UNIVERSITY

in partial fulfillment of
the requirements for the
degree of

DOCTOR OF PHILOSOPHY

June 1965

APPROVED:

Redacted for privacy

Professor of Oceanography

in Charge of Major

Redacted for privacy

Chairman, Department of Oceanography

Redacted for privacy

Dean of the Graduate School

Date thesis is presented April 20, 1965

Typed by Betty Thornton

ACKNOWLEDGMENT

I wish to gratefully acknowledge the encouragement given me by my major professor, Dr. Wayne V. Burt, Chairman of the Department of Oceanography.

Informal discussions with Dr. June G. Pattullo regarding the descriptive physical oceanography of the Oregon coastal waters were both rewarding and stimulating. My thanks go to her and others of the staff of the Department of Oceanography for their assistance.

Additionally appreciated was the assistance given by members of the staff of the Statistics Computing Laboratory at Oregon State University and Mrs. Sue Borden of the Department of Oceanography with problems encountered in programming for the computations performed in this study.

I include acknowledgment and deep thanks to my wife, Gail, for her encouragement and her time spent in typing rough drafts of this thesis.

This study was supported financially by the Office of Naval Research, United States Navy (Contract Nonr 1286(10)).

TABLE OF CONTENTS

LIST OF FIGURES

LIST OF TABLES

CLIMATE AND HEAT EXCHANGE IN THE OCEANIC REGION ADJACENT TO OREGON

INTRODUCTION

The Problem

Man has always been intrigued and affected by climate and the factors which determine it. Until some future time when the inhabitants of this planet have achieved techniques of environmental control, the natural character of particular climatic regions will continue to play a dominant role in the determination of how and where all forms of life exist on earth.

According to Webster's Dictionary (44), climate is "the prevailing or average weather conditions of a place, as determined by the temperature and meteorological changes over a period of years." Climate is influenced mainly by three factors: latitude, the topography of the earth's surface, and the distribution of land and sea. The second and the third of these factors are of particular interest to oceanographers inasmuch as continental topography affects the physical characteristics of the oceans, and these in turn have influence on the climate over both the oceanic regions and the adjacent continental regions.

The oceans have a large thermal capacity. Heat received at the sea surface is slowly distributed into the depths during the heating season and released during the cooling season. This thermal inertia accounts for two important environmental processes. The heating and cooling cycles below the surface are out of phase with the cycle at the surface, and the cycle of storage and release of heat at the air-sea interface tends to modify the climate of adjacent land masses.

Land masses may themselves influence the meteorological-oceanographic processes that are affecting their climate. Continental boundaries are responsible for the configurations and intensities of many important oceanic current systems. These frequently result in climatologically important movements of warm and cool water masses. An example is the Gulf Stream system. The North American continent acts as a barrier to the general circulation of the North Atlantic Ocean, and causes an intensification in the northward flow of warm waters along the east coast of the United States.

Another instance where continental proximity alters oceanographic processes is when surface waters are driven away from land barriers by prevailing winds. The surface waters are then replaced by deeper waters of a cooler and more saline nature. This process, frequently termed "upwelling" (32), occurs along the west coast of North America, particularly along southern Oregon and California.

Other known locations of upwelling are in the coastal waters of Peru, East Africa, Southwest Africa, and France (46, p. 268).

In recent years, several studies of the nature of the upwelling process off Oregon have been made (9, for example). The upwelling process; how, where and when it occurs; and how it affects other oceanographic processes are, however, still not thoroughly understood in the Oregon coastal region.

The purpose of the study described in this thesis was to examine the effects of upwelling on the climatic factors associated with the air-sea interface in the oceanic region bordering Oregon, the relative influence of these effects on the climate of the adjacent land mass, and heat storage and release in the upwelling region.

Region of Study and Data

Geographic Description and Nature of the Data

The region chosen for this study is located between $40^{\circ}00'$ and $50^{\circ}00'$ north latitude, and between the coast of northwest North America and $130^{\circ}00'$ west longitude. This area, henceforth called the Overall Region (Fig. 1), coincides with one of the 10-degree "squares" into which the U. S. Weather Bureau sorts the weather observations reported by vessels at sea. These reports are available from the National Weather Data Center in Ashville, North Carolina,

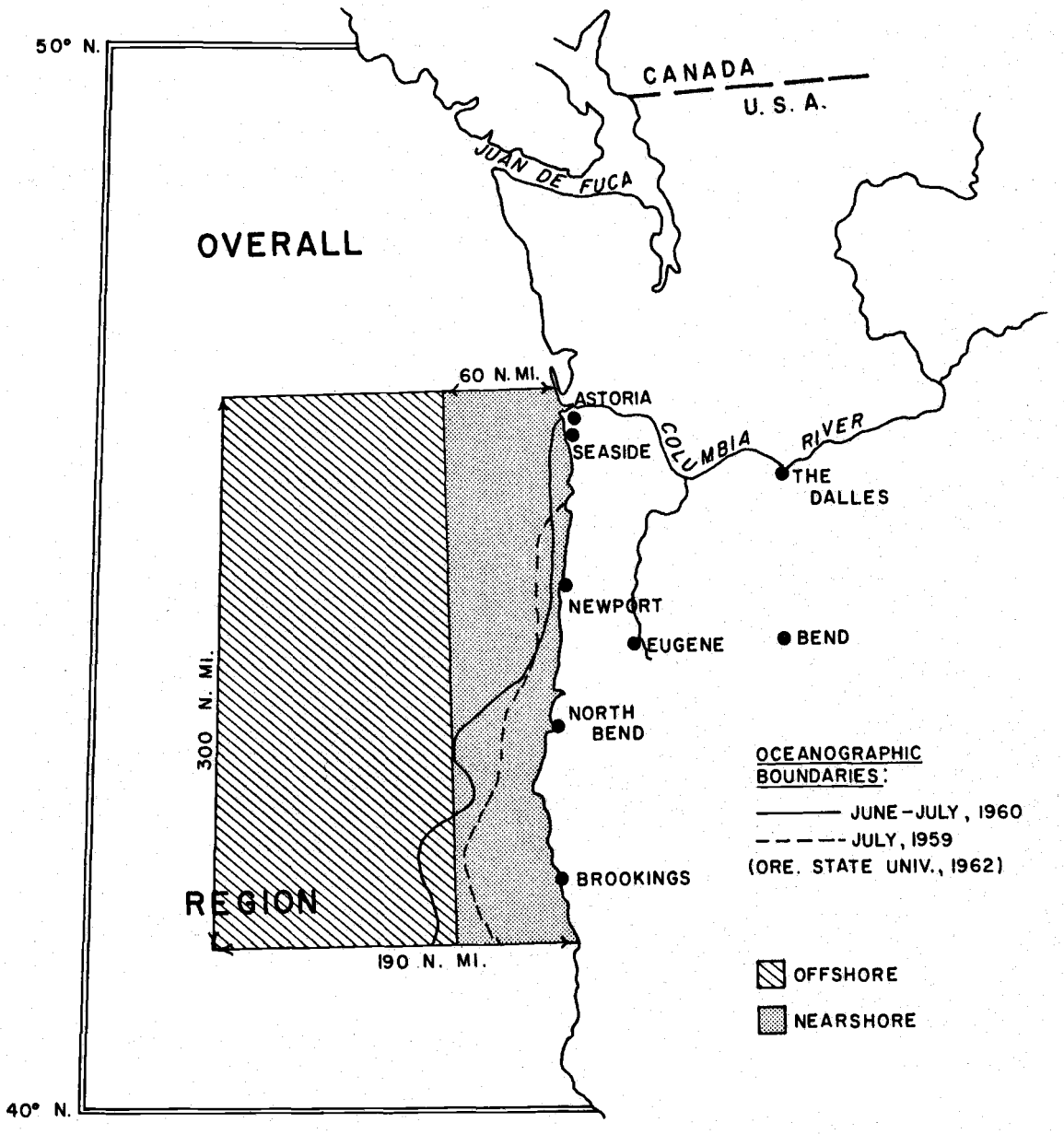

Figure 1. Map of the northwest coast of the United States, including the Overall Region, the nearshore and offshore sub-regions (see text), and the locations of sites referred to in the text.

and are categorized as merchant vessel reports (from 1949), naval vessel reports (from 1952), and British marine reports (1856 to 1953).

Weather reports from the oceanic region along the coast of Oregon are also available from oceanographic expeditions of the Department of Oceanography at Oregon State University. Although these data may be assumed to be consistently well taken, it was decided to use the naval vessel reports for this study for the following reasons: 1) they cover a long period of time (1952 to 1962, inclusive), 2) they are the only data from the Records Center that have had some quality control imposed upon them, and 3) their quantity was large enough for a statistical study (about 30,000 observations). Although the quality of these data may not be as consistently good as those from the oceanographic cruises, their quantity and the length of the period they cover make them preferable for this study.

Solar radiation data, for use in the examination of air-sea heat exchange, was obtained from the Astoria, Oregon, U. S. Weather Bureau Station (Fig. 1) (40).

Meteorological and Oceanographic Conditions

In winter months, the region of study is generally covered by an atmospheric low pressure area (Fig. 2), centered in the Aleutian region. Throughout this period, a succession of frontal storms

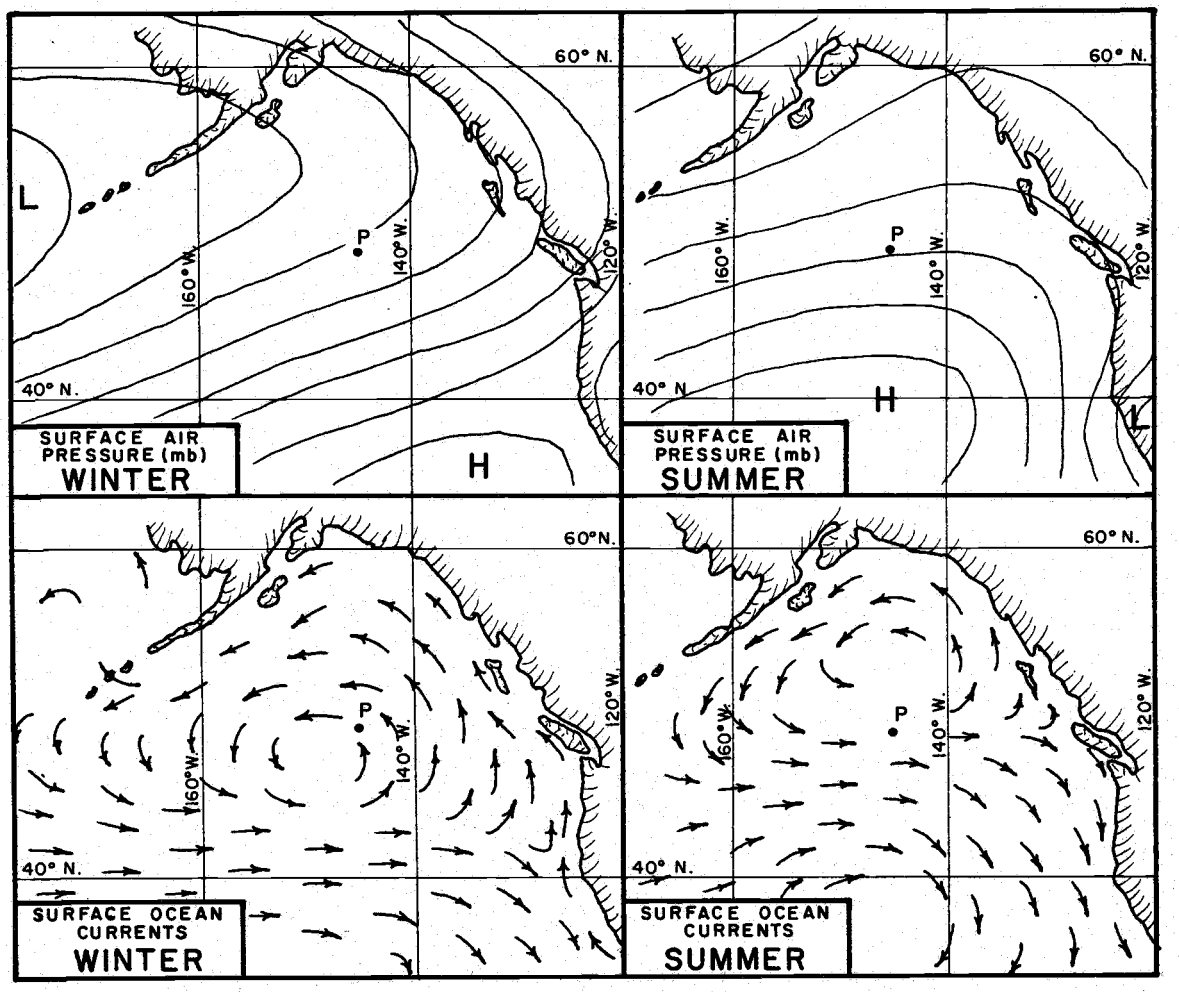

Figure 2. Winter and summer surface air pressure charts and ocean current directions, and the position of Ocean Weather Station "P", in the Northeast Pacific Ocean.

passes through the Gulf of Alaska onto the North American continent, resulting in a predominance of southerly winds and precipitation (14). The regional oceanographic situation features the permanent California Current flowing southward along the United States but separated from the coast by a northward flowing stream, the Davidson Current (35, p. 725). The Davidson Current is generated and maintained by the southerly winds and the action of the Coriolis force moving the surface waters to the right toward the shore, where it concentrates in a band moving northward up the coast (17, p. 86).

In summer months a large high pressure area covers the northeast Pacific (Fig. 2), and the region of study is subjected to a preponderance of northerly winds. Frequently, the high pressure area extends into the northern part of the western United States and the wind along the Oregon coast becomes northeasterly. With either northerlies or northeasterlies, the effect of the Coriolis force is to drive surface waters away from the coast. Except for the strong discharge from the Columbia River and Juan de Fuca Strait (Fig. 1) in mid-summer, coastal runoff is low and upwelling may occur, especially south of the Columbia River (Fig. 3) (9). The local occurrence of the cool, upwelled water promotes the formation of fog, especially when the overlying airflow is warm, as when an offshore flow occurs (21).

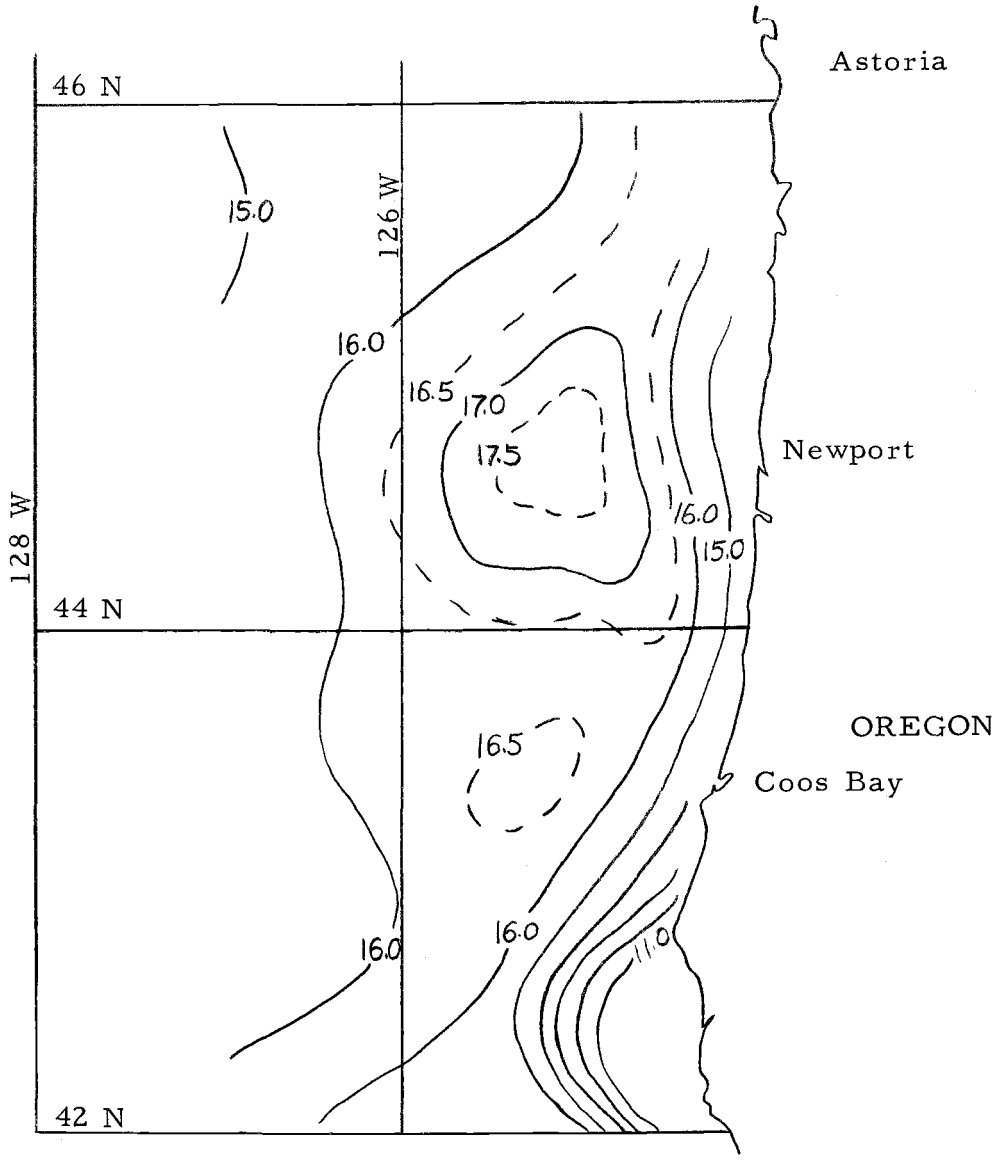

Figure 3. Sea surface temperature (°C) off Oregon (cruise of 30 June to 9 July 1959) (26).

It should be noted that the pattern described above is one of average conditions. That is, in summer there is a predominance of northerly winds, hence upwelling; while in winter there is a predominance of southerly winds, hence convergence. When examined closely, it is seen that any one season is subject to variations from one pattern to the other. Thus, it may be expected that conditions favorable for upwelling will occur during part of the winter season, but for the season as a whole, the convergence pattern will prevail. Examples will be presented in subsequent sections to demonstrate seasonal trends.

The Sub-regions

The eleven years of data used in this study were analyzed by months. If the data were uniformly distributed in time, there would be more than 200 observations per month. However, there were large variations in numbers of monthly observations, and one month (May, 1955) had no data available. There is also no reason to expect that the observations were uniformly distributed in space. This is a more serious problem, as spatial variations over the area of the Overall Region were expected to be larger in magnitude than local variations over the period of one month. For this reason, and to accommodate the purpose of studying upwelling, two sub-regions

were chosen for the detailed portions of this investigation. The subregions are shown in Figure 1 and constitute a "nearshore" upwelling region and an "offshore" region. Also shown in this figure are the boundaries of two summer upwelling regions, determined from hydrographic data (25).

CLIMATOLOGICAL FACTORS

Description and Significance

Many parameters are involved in the description of the total climate of a region. In this study, only those parameters which are important to the exchange of heat between the sea and atmosphere are included. These include sea surface temperature, temperature and moisture content of the air above the sea, wind speed, and cloud cover.

An example of the data reports used in this study is shown in Figure 4. All of the weather observations were coded on IBM cards, suitable for use by the IBM 1620 computer at the Statistics Computing Laboratory, Oregon State University. Each data card contained more data than was necessary for the study, and those items which were used are indicated in Figure 4. Because of the way in which some of the data is coded in the weather report, is is impossible to use a normal programming technique (FORTRAN II) in reducing the data to averages. A member of the staff of the Statistics Laboratory was asked to write a "machine program" for averaging items of interest from each month's set of data.

Throughout this thesis, data are analyzed by months. For each month (for example, June, 1959), there were several available

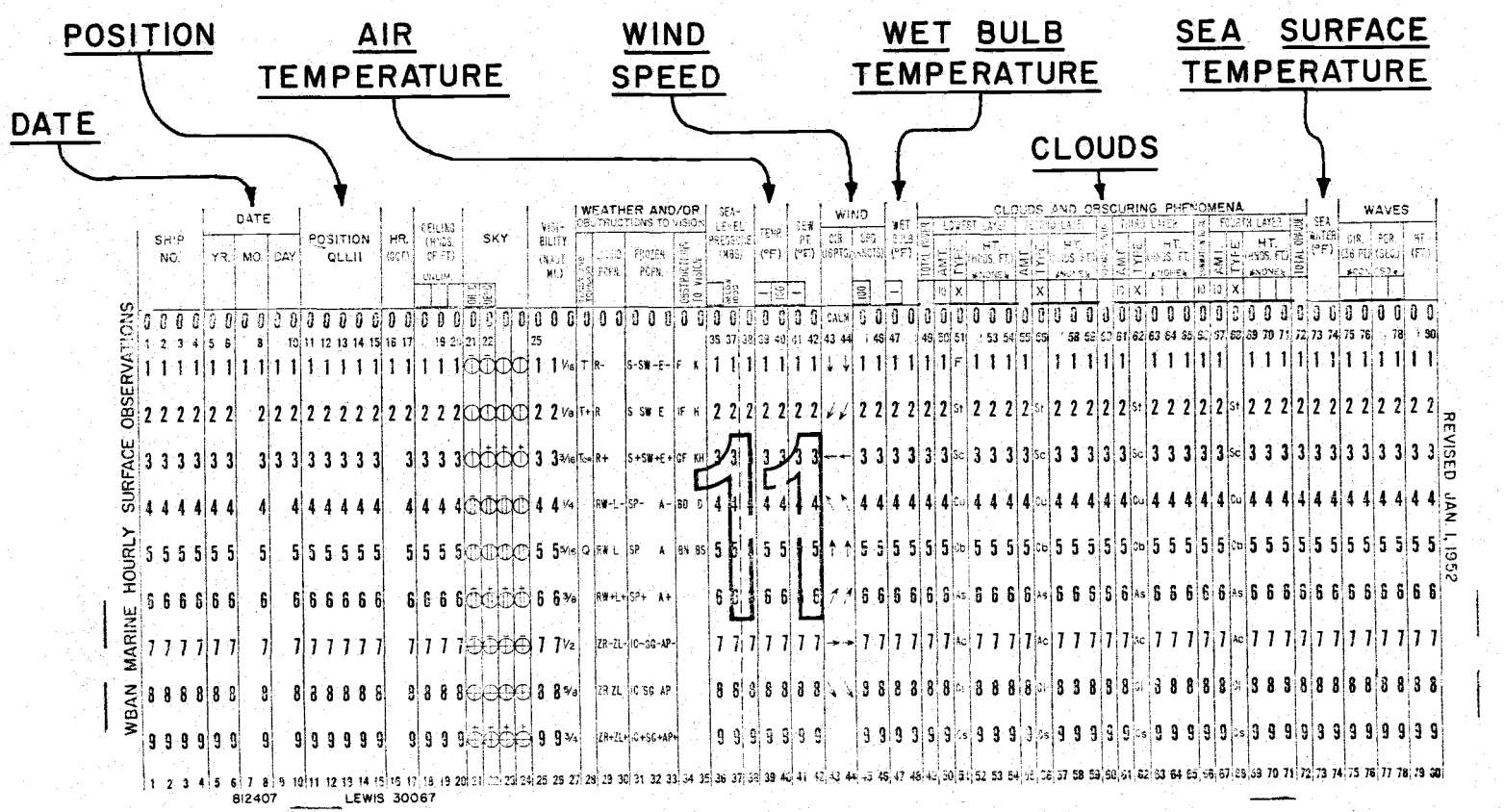

Figure 4. Example of data card, showing terms used.

observations of each parameter being analyzed. These observations were averaged to obtain individual monthly values called averages, and all the individual averages (for example, all the June averages) were averaged to obtain monthly means. The means referred to in the thesis are taken to represent long term mean conditions for each month.

Sea surface temperature (T_s) (see Appendix for meanings of symbols) may be measured from a ship by several techniques. Merchant vessels use thermometers mounted in the water intake for engine room use. Because of the poor location, the temperature sensor may be adversely influenced in this method. Oceanographic and naval vessels, which frequently use an oceanographic instrument (the bathythermograph (30)) to obtain temperature soundings, generally obtain surface temperature values by securing a bucket of water from the sea surface and using a deck thermometer placed in the bucket.

The temperature of the air (dry bulb temperature, T_a) is normally measured at bridge level (about 6 meters above the sea surface) in a ventilated shelter where the thermometers are shielded from the sun.

In addition to the standard thermometer, the instrument shelter mentioned above normally contains a thermometer whose sensing bulb is covered with a muslin wick. When the wick is moistened,

evaporation saturates the air near the bulb and the temperature drops because of the release of latent heat. The temperature at saturation is the "wet bulb" temperature, T_w, and will equal the dry bulb temperature only when the environmental air is saturated. The value of $(T_a - T_w)$ is the "wet bulb depression" (13, p. 27).

Wind speed (V) measurements at sea are certain to be less accurate than land measurements of wind. The velocity of the ship is estimated, then subtracted vectorally from the indicated wind velocity. Also, the rolling and pitching of the vessel cause sudden accelerations of the anemometer through the air and introduce unreal fluctuations in the readings. Most of the numerical work in this study involves comparisons of similarly obtained data. Hence, by assuming that shipboard wind measurements are somewhat consistently taken, their use either by themselves or when V is a linear parameter in empirical equations is justifiable.

The fraction of sky obscured by clouds (c) is estimated (in tenths) by a single observer at a position. This parameter is most useful when used statistically with a large number of observations. Cloud cover is frequently used to determine the fraction of possible insolation which reaches the surface. An individual observation of c tenths of cloud cover does not indicate whether the sun was ever (or never) shielded from the observer's position over some period of

time, nor does it say how thick the clouds were. It is considered valid, however, to assume that a monthly average c indicates that the sun was shielded c tenths of the time during all parts of the day. The use of such a monthly value in empirical equations generally assumes some average thickness of clouds.

A standard meteorological observation includes an estimate of the height of all visible cloud layer bases. In this study, the height of the cloud layers (h) is used in an empirical equation for estimating long wave radiation from clouds. Each data card (Fig. 4) contains data for a maximum of four layers of clouds. When averaging the values of h, the computer was instructed to "examine" each set of cloud data, beginning with the lowest layer and proceeding to successively higher layers. The height selected for a particular observation was that of the layer at which the total of the c values, summed over the preceding layers, became greater than 5. If the total of all the layers was less than or equal to 5, the h value for the highest layer was chosen.

The remaining climatological factors considered were vapor pressures. Immediately above the air-sea interface, the air is presumed to be saturated with water vapor. The number of molecules of water vapor present is a function of the activity of the surface water molecules, which is a function of the water temperature. The

Clausius Clapeyron equation

$$\frac{1}{e_s}\frac{de_s}{dT_s} = \frac{L}{R_v T_s^2} \qquad (1)$$

may be used to calculate the saturation vapor pressure, e_s, when T_s and the slope of the e_s versus T_s curve are known. L is the latent heat of vaporization, and R_v is the gas constant for water vapor. The saturation vapor pressure over sea water having chlorinity Cl is lower than it is over a surface of distilled water, at the same temperature. The difference is determined from the equation (35, p. 67)

$$e_s = (1 - 0.000969\ Cl)\ e_d, \qquad (2)$$

where e_d is saturation vapor pressure over distilled water, and is insignificant when one considers the lack of precision in obtaining the value of T_s.

At a height above the surface where the air is not saturated with respect to water vapor, the vapor pressure e_a is lower than e_s at the air temperature. Integrating the First Law of Thermodynamics for the wet bulb process (described earlier) and introducing suitable approximations for the mean mixing ratio (13, p. 26) give

$$\frac{T_a - T_w}{e_w - e_a} = \frac{0.622\ L}{c_p p}, \qquad (3)$$

where c_p is the specific heat at constant pressure and e_w is the

saturation vapor pressure at the wet bulb temperature. By rearranging and letting the atmospheric pressure, p, equal 1000 millibars,

$$e_a = e_w - \frac{(T_a - T_w)\, 1000\, c_p}{0.622\, L} \qquad (4)$$

The Clausius Clapeyron equation (1) is used with T_w to determine e_w. An atmospheric pressure of 1024 millibars would result in a 2 percent error when $(T_a - T_w)$ is 3 C^o.

The Climate of Western Oregon

The climate along the northwest coast of the United States is described by Haurwitz and Austin (14, p. 118) according to the Köppen classification, as either Cf (warm temperate rainy without a dry season) or Cs (warm temperate rainy with a summer dry season). A short distance inland from the coast the climate is more complex, being affected by the intricate mountain and valley systems. Climatic conditions in Oregon east of the Cascade Range are much different from the coastal regions (temperature ranges are much larger and annual precipitation is much smaller). In all these regions, there are north-south variations of the climatic parameters, but the striking changes are in the east-west sense.

Distributions of some of tne climatic indicators are shown in Table I. The list contains selected Oregon stations (see Fig. 1 for their locations) with the long-term averages of their extremes of mean monthly temperatures and their total annual precipitation. The coastal stations (Astoria, Newport, North Bend, and Brookings) have a temperature range of 3.8 F^{o} in their extreme monthly maximum temperatures and a range of 6.9 F^{o} in their extreme monthly minima. The temperature ranges (extreme monthly maximum and minimum) found in the data from the west-east line of stations, Newport-Eugene-Bend, are 8.6 F^{o} and 13.2 F^{o}, respectively. The range in values of total annual precipitation in these coastal stations is 19.5 inches while the range for the west-east line is 52.5 inches. The uniformity of the coastal climate and its contrast with the climate a short distance inland are demonstrated by these values.

Table I. Climatological data from selected Oregon stations.
A. highest value of the long term mean monthly air temperatures
B. lowest value of the long term mean monthly air temperatures
C. mean annual precipitation

	A.	B.	C.
Astoria	61.8 ^{o}F	40.1 ^{o}F	76.0 inches
Newport	58.0 ^{o}F	43.7 ^{o}F	64.8 inches
North Bend	59.6 ^{o}F	45.2 ^{o}F	62.3 inches
Brookings	59.1 ^{o}F	47.0 ^{o}F	81.8 inches
Eugene	66.6 ^{o}F	38.2 ^{o}F	37.5 inches
Bend	63.7 ^{o}F	30.5 ^{o}F	12.3 inches

THE CLIMATE AT THE AIR-SEA INTERFACE

Overall Region: Description of the Climate

The monthly averages of air temperature T_a, wet bulb temperature T_w, and sea surface temperature T_s obtained from the 11 years of data for the Overall Region are shown in Figures 5 and 6. Figure 6 also contains a comparison of the monthly means of these values. The means of the monthly averages indicate that the peaks of the T_a, T_w, and T_s cycles occur in August, and that the peak of the T_s cycle is definitely flatter than those for the other temperature cycles. For individual years, the number of times in the 11 years studied that the peaks occurred in August, September, and October are T_a (8, 3, and 0); T_w (7, 3, and 1); and T_s (4, 6, and 1), respectively. Therefore, despite the mean curves shown in Figure 6, the peak T_s values occurred more frequently in September, generally later than the T_a peak values. This is contrary to the findings of Tabata (36) at Ocean Station P (Fig. 2) which indicated that T_a and T_s values peaked during the same month in the three years he studied.

Although summer values of T_a are higher than those of T_s (Fig. 6), winter values are lower. The minima in the annual cycles of T_a, T_w, and T_s are less sharply denoted than the peak values (Fig. 6). For individual years, the number of times that the minima

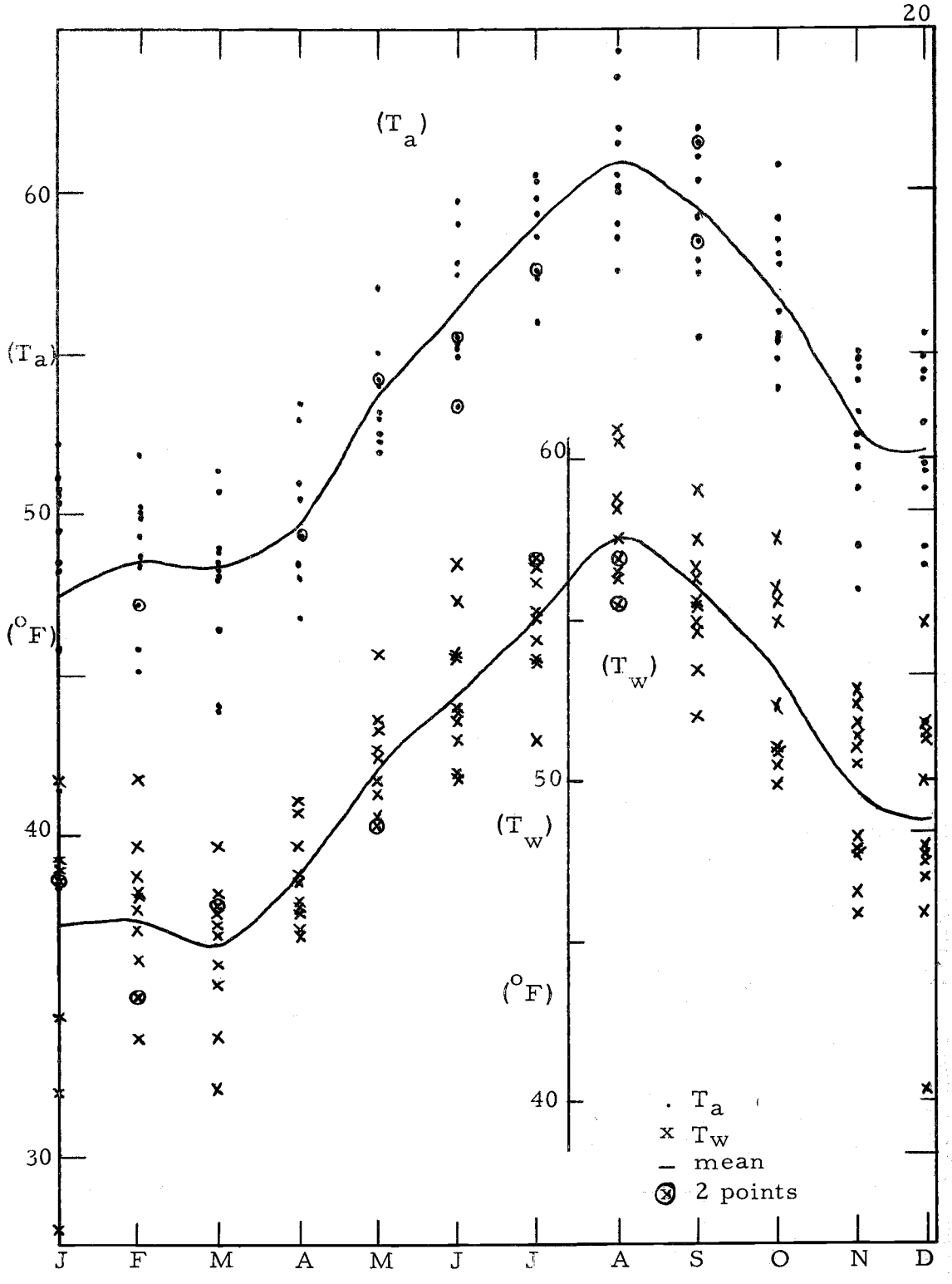

Figure 5. Monthly averages of air temperature (T_a) and wet bulb temperature (T_w) for each of the years studied, and the means of the sets of averages for the Overall Region.

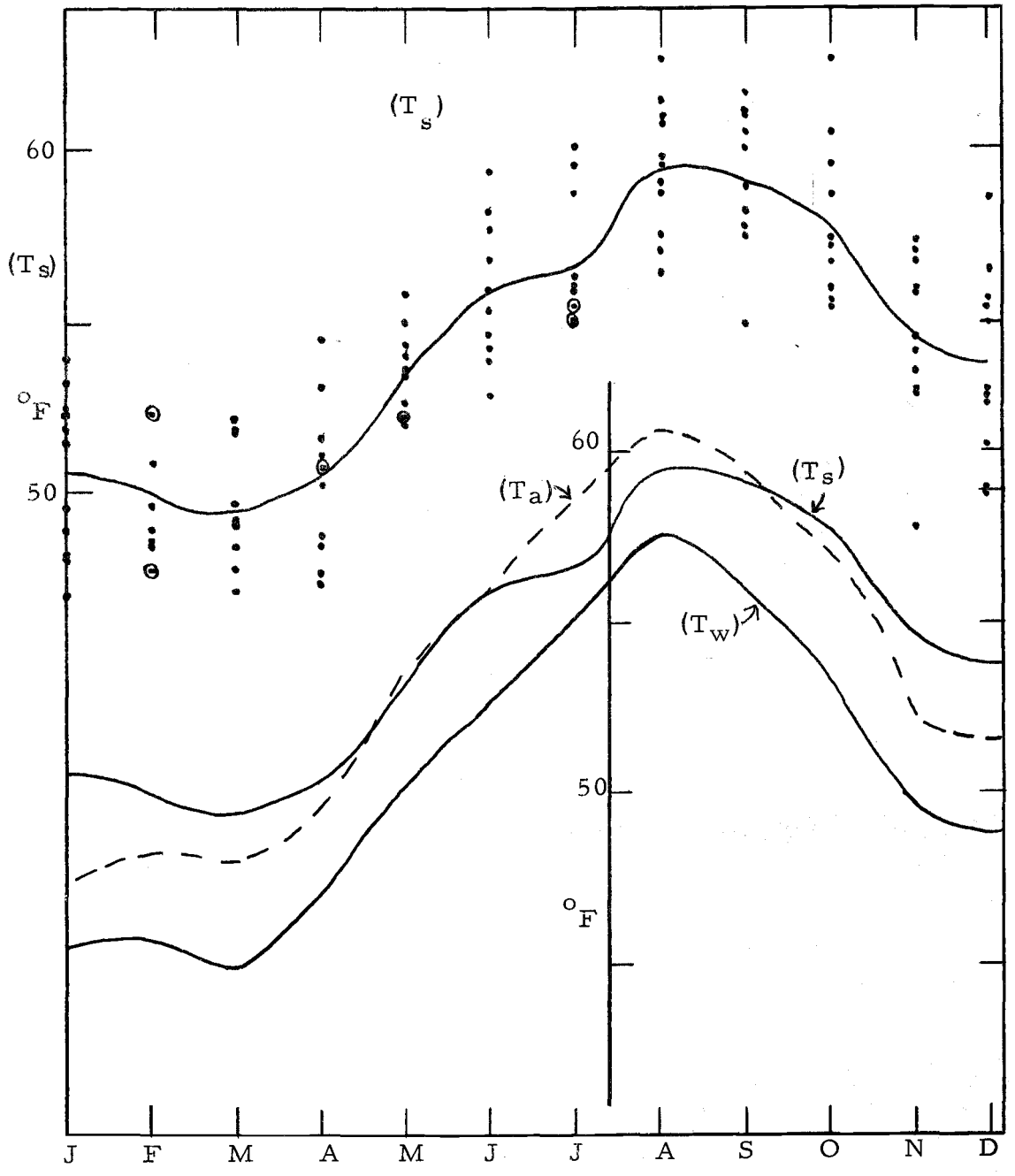

Figure 6. Monthly means of sea surface temperature (T_s) for each of the years studied, the means of these averages, and a comparison of the means of T_a, T_w, and T_s (see Fig. 5) for the Overall Region.

occurred during the months of December, January, February, March, and April, respectively, are: T_a (1, 3, 3, 4, 0); T_w (1, 2, 3, 5, 0); and T_s (0, 4, 1, 2, 4). Here again, minimum values of T_s generally occurred later than did those of T_a.

Monthly averages and their means, of wind speed and cloud cover, obtained from the data for the Overall Region are shown in Figure 7. Figure 8 contains plots of monthly averages, and their means, of the atmospheric vapor pressure, e_a; the saturation vapor pressure at the mean of the average monthly air temperatures $(e_s)_a$; the saturation vapor pressure at the sea surface temperature (e_s); the wet bulb deficit $(T_a - T_w)$; and the relative humidities (R. H.) obtained from the monthly ratios of $(e_a)/(e_s)_a$.

Cloud cover (Fig. 7) appears to vary little throughout the year, with the main scatter of values being between 5 and 8 tenths of sky covered. There is a trend to a winter high and an autumn low in the slight cycle that is evident in the mean values.

There is a rather large scatter in the monthly averages of wind speed (Fig. 7). The seasonal cycle shown by the mean values does, however, clearly indicate a summer minimum and a winter maximum; the range being about 4 knots. It is interesting to note that the range in monthly averages from the years examined is highest in winter months (16.5 knots in January, 15 knots in February) and lowest in

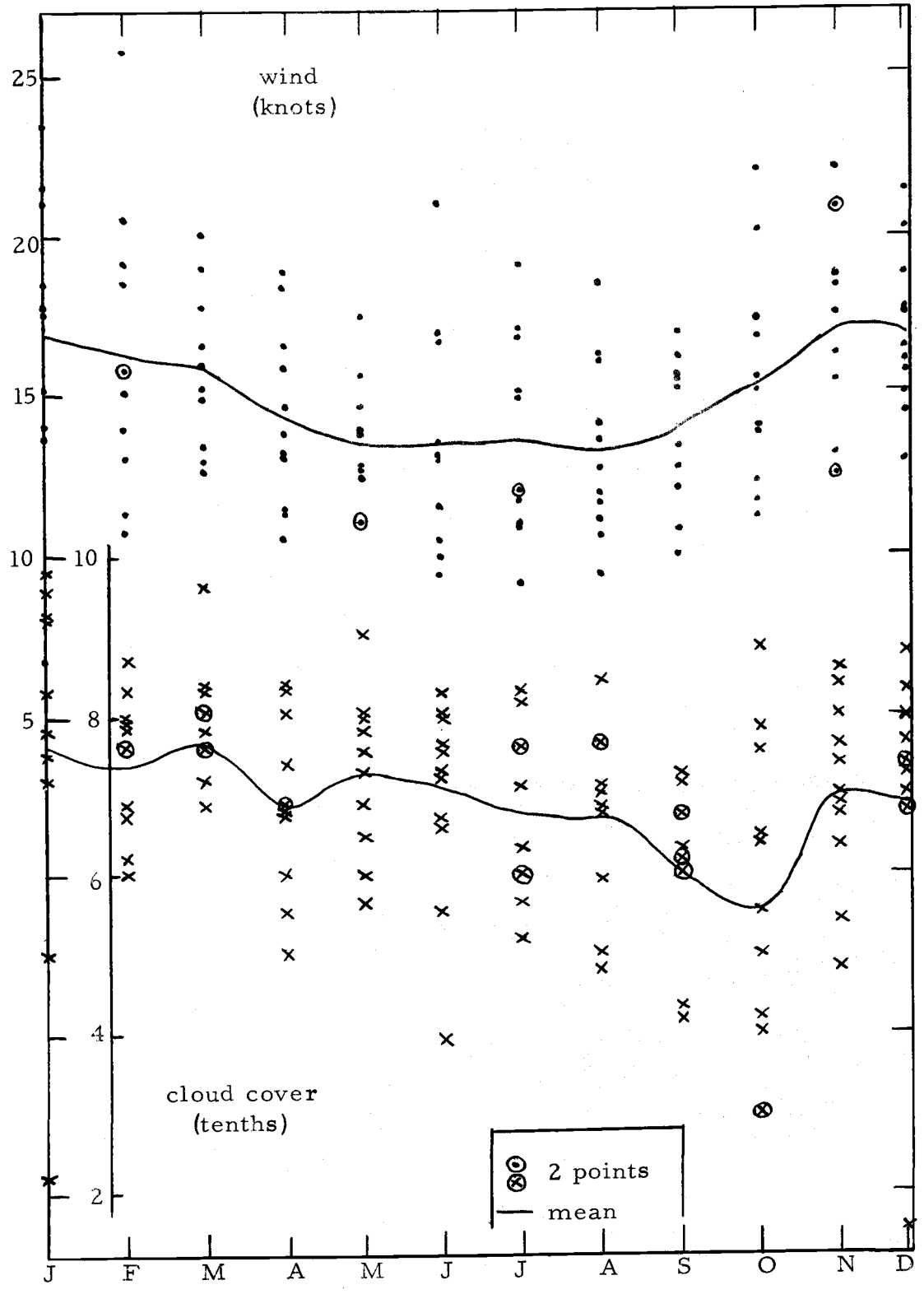

Figure 7. Monthly averages (and the mean) for the years studied of wind speed V, and cloud cover c, for the Overall Region.

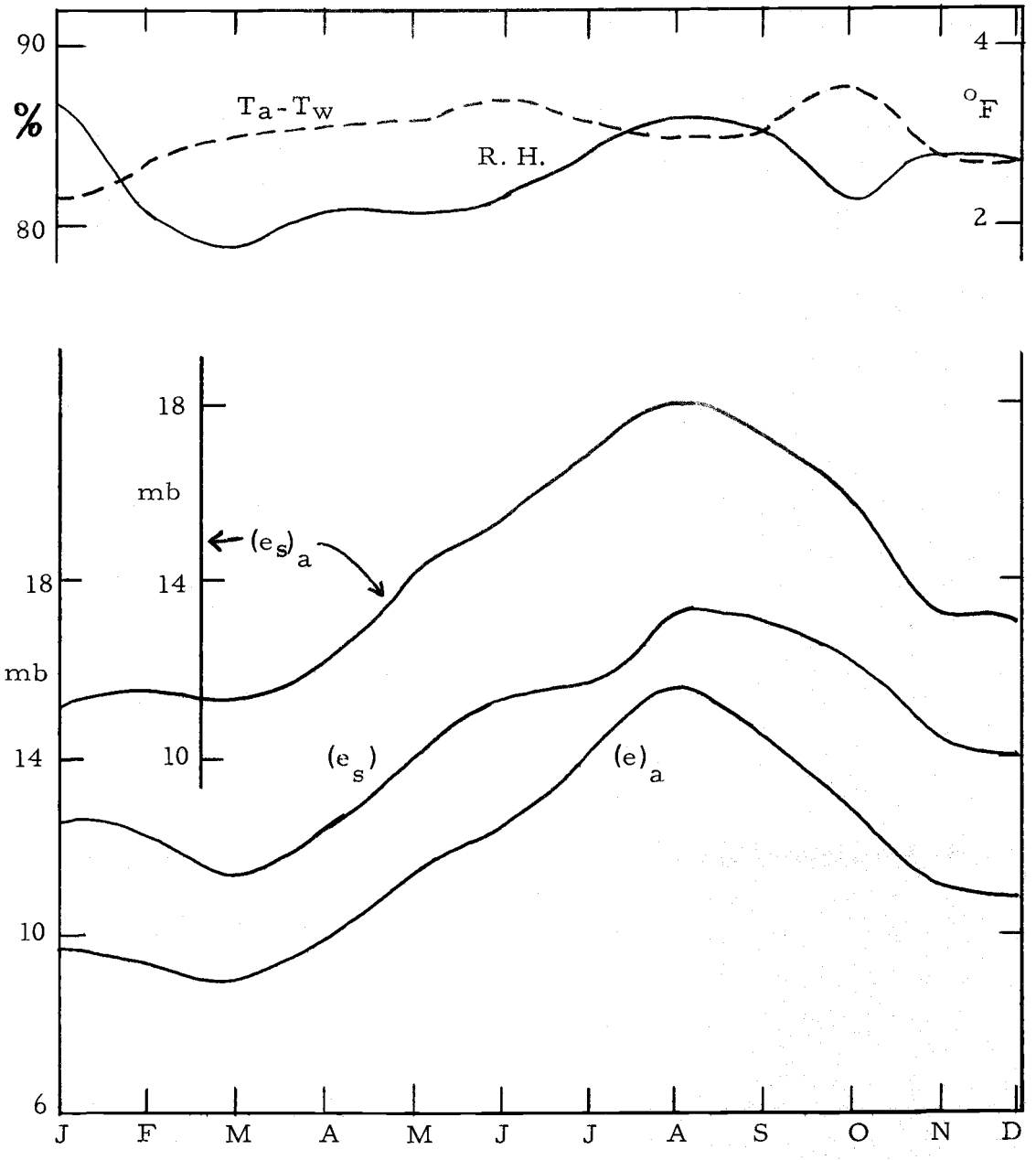

Figure 8. Monthly averages (and the mean for the years studied of atmospheric vapor pressure, e_a, saturated vapor pressure at the sea surface, e_s, saturation vapor pressure at the air temperature, $(e_s)_a$, relative humidicity, R. H., and the wet bulb deficit, $(T_a - T_w)$ for the Overall Region.

the spring and autumn months (6.5 knots in May, 7 knots in September).

The atmospheric vapor pressure, e_a (Fig. 8), follows the summer high and winter low cycle expected from the similar air temperature pattern and the relatively consistent wet bulb deficit. The latter varied from 2.3 to 3.5 F^o and showed a slight trend to lower winter values. Relative humidity (monthly means) also had a small range of values, varying from 79 to 87 percent.

Overall Region: Discussion of the Climate

In early summer, solar heating results in a rise in the values of both air and sea temperatures. In the Overall Region, as in the Gulf of Alaska at Station P (36) and the coastal region of Vancouver Island (28) air temperatures generally exceed sea surface temperatures in the summer months. There are several reasons which contribute to this condition. The main flow of air, represented by storm tracks (39, charts 52, 60, and 72) in June, July, and August, is from the southwest into the Gulf of Alaska, then down to the region of this study. As this warm air approaches the Gulf of Alaska, it crosses a relatively cool water mass so that the air-sea temperature difference ($T_a - T_s$) is high and positive (39, chart 68). By the time this air reaches the Overall Region, this difference is less but still positive. As pointed out in a previous section, the air flow over the

Overall Region is predominantly from the northeast during periods in the summer months. Such contributions of continentally warmed air will serve to increase the air-sea temperature difference. A further, though probably less important (to the entire Overall Region), contributor to this difference is the cooling of nearshore waters in the Overall Region due to coastal upwelling.

In early autumn the cooling cycle begins and air temperatures drop. The mean air temperature (Fig. 6) remains slightly higher than the sea surface temperature, allowing the latter to continue to rise for a short period following the peak of air temperatures. During the remainder of the cooling season, air temperature values decrease to below those of the sea surface. Tabata (36) found that winter values of air and sea surface temperatures at Station P were very close and that sea surface temperature values may remain lower throughout the cooling season. Pickard and MacLeod (28), however, found that the nearshore waters along the coast of Vancouver Island were warmer than the air during the winter. It appears, therefore, that in the Northeast Pacific this phenomenon is associated with the coastal locale. The difference in specific heats, of course, favors a slower decrease in sea temperatures, but there is evidently some characteristic of the coastal system which explains this difference in the relationships between the temperature cycles. This will be

considered in the analysis of the heat budget.

The amount of cloud cover is of considerable importance to the climate of an oceanic region; the amount of solar radiation and the amount of long wave radiation reaching the sea surface depend upon it. It is seen from Figure 7 that the variation in values within each single month is great enough to make the slight seasonal variation relatively unimportant. This is rather surprising when it is considered that the summer months are generally influenced by an atmospheric high pressure system, which normally would indicate a trend to small amounts of cloud cover. Winter months are generally influenced by the passage of low pressure systems and storm fronts. It is seen, however, that in the mean case, the saturation vapor pressure at the sea surface is always greater than the atmospheric vapor pressure above the water. This indicates that in the mean situation the process of evaporation is always taking place. This situation, in turn, explains the consistently high amount of cloud cover, an occurrence which is not limited to just the coastal region of the Northeast Pacific (39, charts 7, 35, 63, and 91).

As in the case of the cloud cover, the monthly range of values of wind speed (Fig. 7) renders the seasonal cycle almost meaningless. The atmospheric pressure systems, which normally occupy the region over the Northeast Pacific, would probably cause a wind

pattern weaker than the one observed in summer if they acted alone. This would result in a more definite winter-summer cycle, featuring the high speeds associated with the passage of winter storms, and the low speeds associated with the presence of the summer high pressure area offshore. The situation is complicated, however, by the summer presence of a strong trough of low pressure, generally centered in southeastern California and extending up the California coast to southern Oregon (39, charts 66 and 78). This low pressure area, called a "heat low" (14, p. 181) results in a strengthening of the pressure gradient along the Oregon and Washington coasts and particularly in the coastal region of southern Oregon.

Annual variations in the values of a particular property may result from a lack of uniform sampling over the large region of study. As pointed out earlier, a large spatial variation may be expected in the Overall Region, as demonstrated in Figure 3 with the use of a single climatic variable, sea surface temperature.

Sub-regions: Description of the Climate

The climatic data from the two sub-regions (Fig. 1) were averaged for each month of the 11 years examined. The monthly means of these averages are shown in Figures 9 and 10. Each figure contains curves representing data from the nearshore upwelling

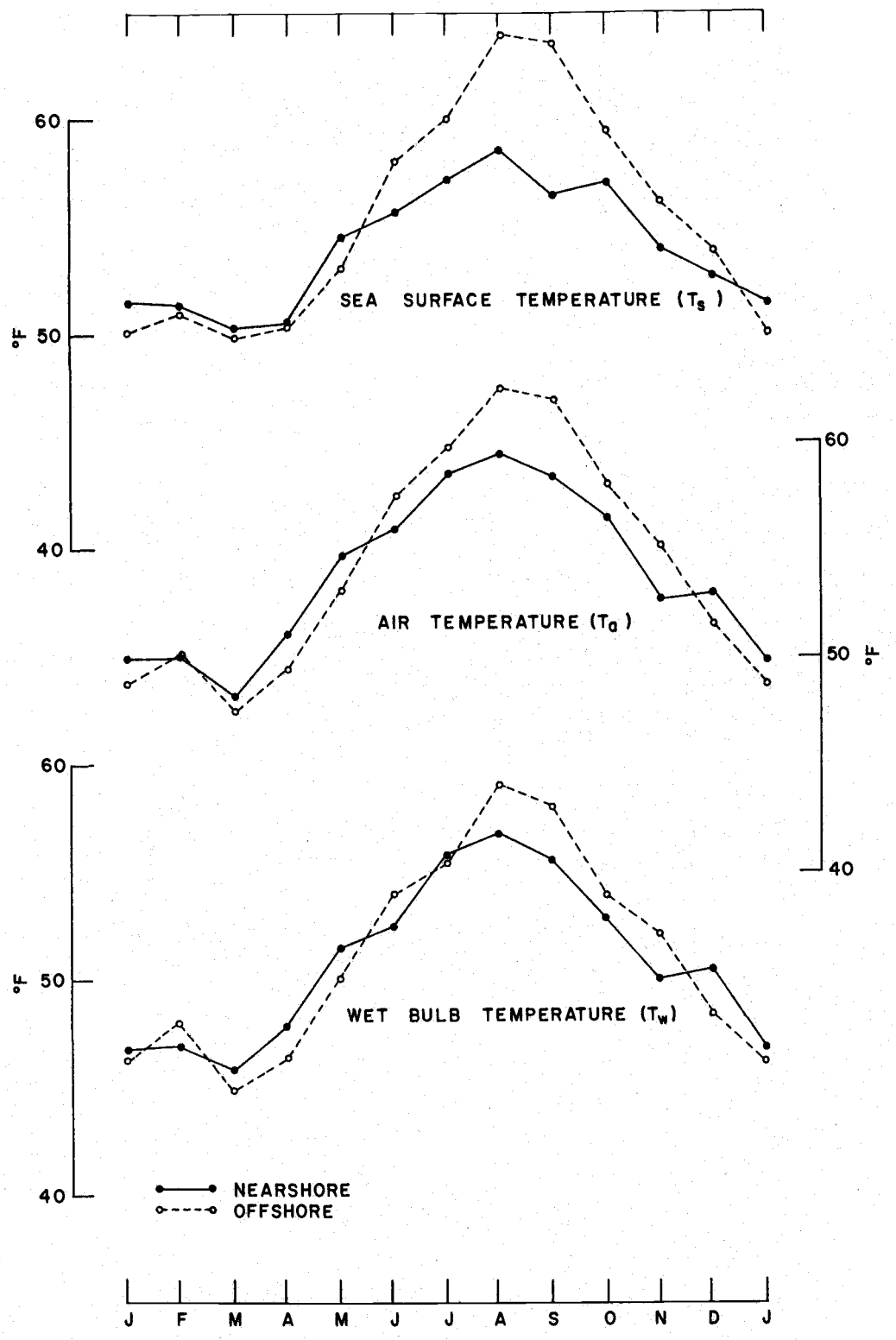

Figure 9. Comparison of temperature means from nearshore and offshore sub-regions: (a) sea surface, T_s, (b) air, T_a, and (c) wet bulb, T_w. Means are of monthly averages of at least 4 observations (1952-62).

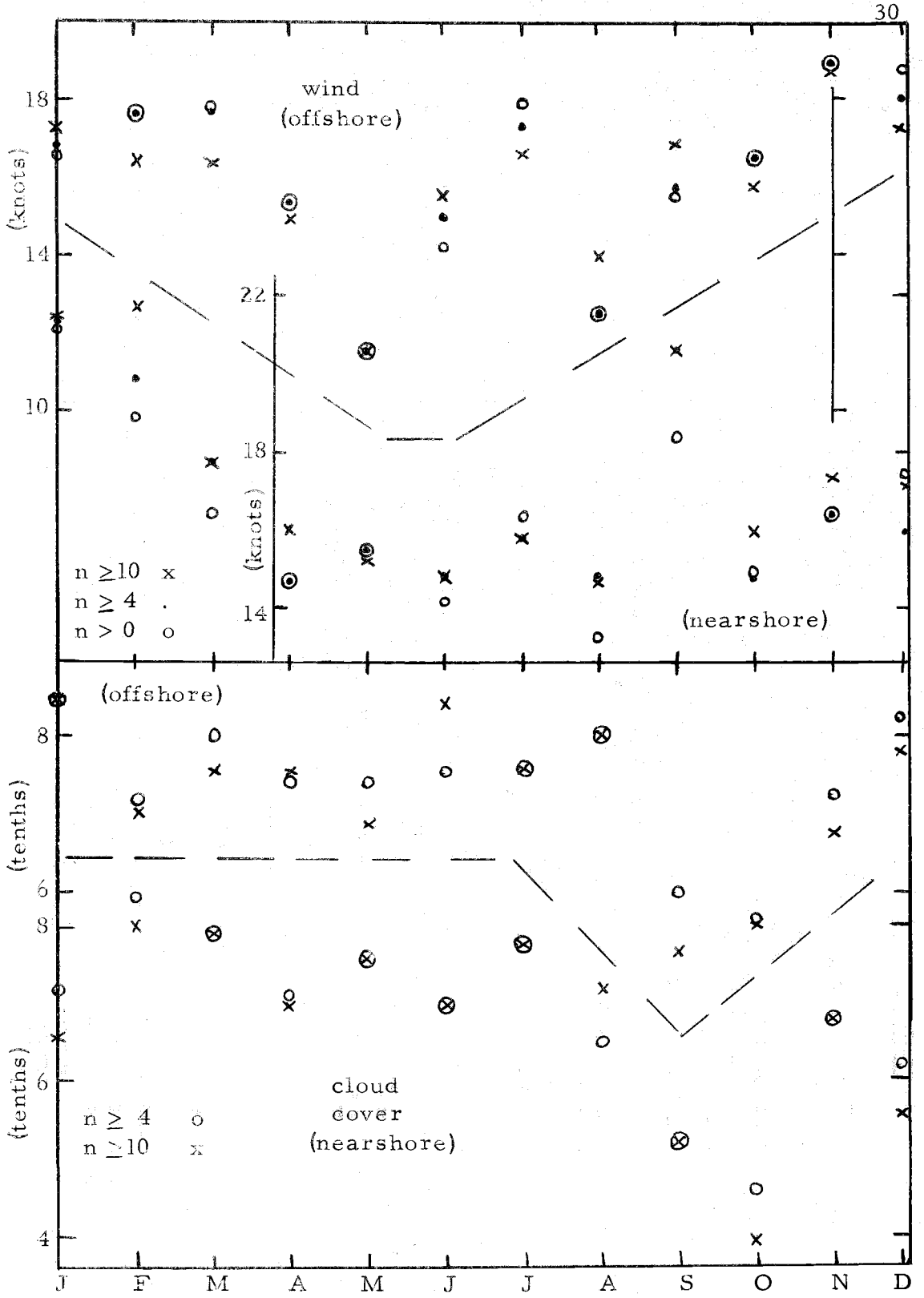

Figure 10. Means of monthly averages from 1952 to 1962 (obtained from months having total of n observations) of wind speed and cloud cover, for the nearshore and offshore sub-regions.

region and one of data from the offshore region.

In separating the data into sub-regions, a large spread in the number of observations per month was noted. This spread ranged from no observations to 262 observations for a particular month in a particular sub-region. Eleven-year means were obtained using all the monthly averages, those monthly averages from four or more data observations, and those from 10 or more observations. It was expected that the averages of cloud amount and wind speed would be adversely affected by too few observations. For example, two or three cloud observations or wind observations can scarcely be representative of an entire month. On the other hand, relatively few air or sea temperature measurements may be assumed to be fairly representative of monthly conditions in a given year. The analysis was complicated by the fact that, by limiting the usable averages in determining the means, some monthly means would have been determined from as few as four averages, and not necessarily the same four as used for other months or the other sub-region.

Plots of air temperature and cloud cover means for both sub-regions were determined from the three sets of averages described above (Fig. 11). Reducing the number of averages of air temperature affected only the December mean and slightly affected the winter trend by introducing a double minimum. Otherwise, the values are

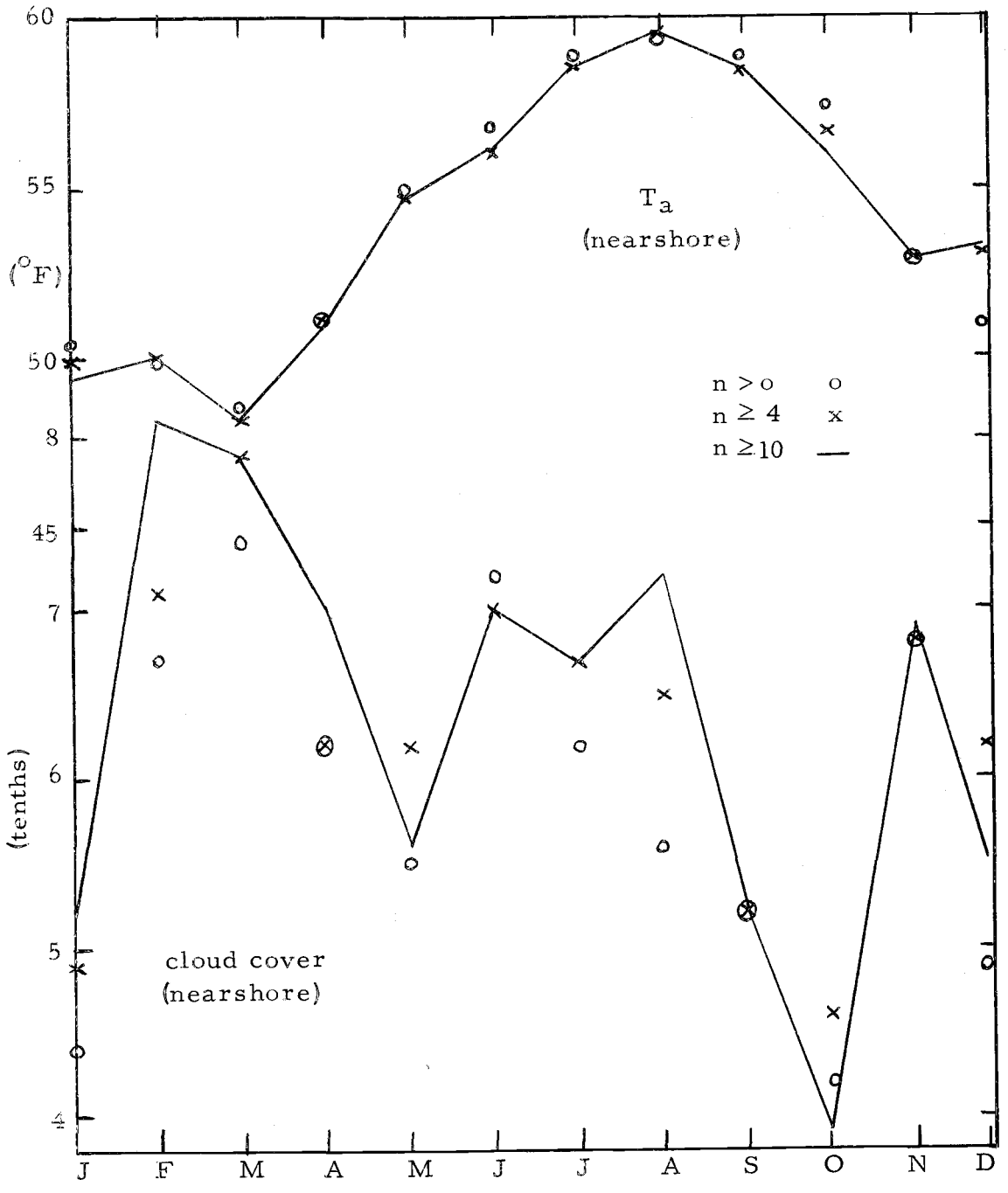

Figure 11. Comparison of averages of monthly means from 1952 to 1962 obtained from n observations for various values of n, of: air temperature, T_a, and cloud cover, c, for the nearshore sub-region.

quite close to one another. On the other hand, the cloud cover means differ within one month from 25 to 40 percent of the annual range. Therefore, all three representationsof the parameters are used in this section. In the quantitative analyses, involving the heat budget computations, cloud and wind data averaged from at least 10 observations were used. Means obtained from data samples with more than three observations were used for analyses of the other parameters.

Eleven year mean values of T_s in the nearshore region are lower than those found in the offshore region for the period June through December (Fig. 9). This difference reaches a maximum in August and September and tapers off gradually in the late months of the year. A weak second maximum is noted in autumn in the nearshore region. During the winter months, the curve of the seasonal cycle is almost level and features a double minimum in the offshore data. From January through May, the values in the offshore region are lower than those of the nearshore region.

The air temperature and wet bulb temperature patterns (Fig. 9) are similar to the pattern of the sea surface temperature. As with the T_s data, the offshore patterns show a double minimum. This is also present to a slight extent in the nearshore T_a and T_w data.

The cloud amount patterns for both sub-regions are shown in Figure 10. There is a definite autumn minimum in both sub-regions.

Through the remainder of the year the mean cloud cover varies around 7 and 8 tenths. Nearshore and offshore data patterns are similar. The autumn minimum of cloud cover was confirmed by an examination of the individual monthly averages. In September, 1961, 62 observations had an average c equal to 3.6 tenths in the nearshore region, and in September, 1958, 56 observations had an average c equal to 4.9 tenths, in the offshore region.

The wind speed pattern for the sub-regions, from the means of the three different sets of averages as defined in the cloud cover description above, are also shown in Figure 10. Although most of the means lie between the limits of 14 and 18 knots, there is a general pattern of lower wind speeds in summer months. In the offshore region, the summer patterns suggest that there are two minima, one in the spring and one in the late summer. The nearshore region has a simpler pattern, except for an anomalous peak in September. In September, 1956, the average of 38 observations of wind speed was 29.1 knots; in 1961, the average of 62 observations was 22.0 knots. Thus, the September mean appears to be valid and not just the result of too small a set of data.

The nearshore monthly means of vapor pressure e_a and saturation vapor pressure at both the sea surface temperature (e_s) and the air temperature $(e_s)_a$ are generally lower in the summer and higher

in the winter than those in the offshore region. The relationships between nearshore and offshore values of the wet bulb deficit, relative humidity, and $(e_s - e_a)$ are shown in Figure 12. Values of the wet bulb deficit and $(e_s - e_a)$ in the winter are generally higher. Generally the values are lower in the offshore region in the summer. As expected from this, the relative humidity shows the opposite relationship.

Sub-regions: A Discussion of the Climate

An examination of the climate of the sub-regions in the previous section has shown a distinct seasonal relationship in the differences between the climatic variables of one region compared to variables of the other region. The reasons for this relationship, since it is seasonal, may be assumed to be meteorological, oceanographic, or both. The magnitude of the oceanographic differences (Fig. 3) between the sub-regions definitely correspond with the nearshore cooling and salinity increase attributed to upwelling (9). The closeness with which the atmospheric changes follow this oceanographic change (Fig. 9) indicates that any possibility that the responsibility for the nearshore-offshore differences lies with some process other than upwelling; for example, a purely meteorological (atmospheric) process such as a local influx of cool air or a localized

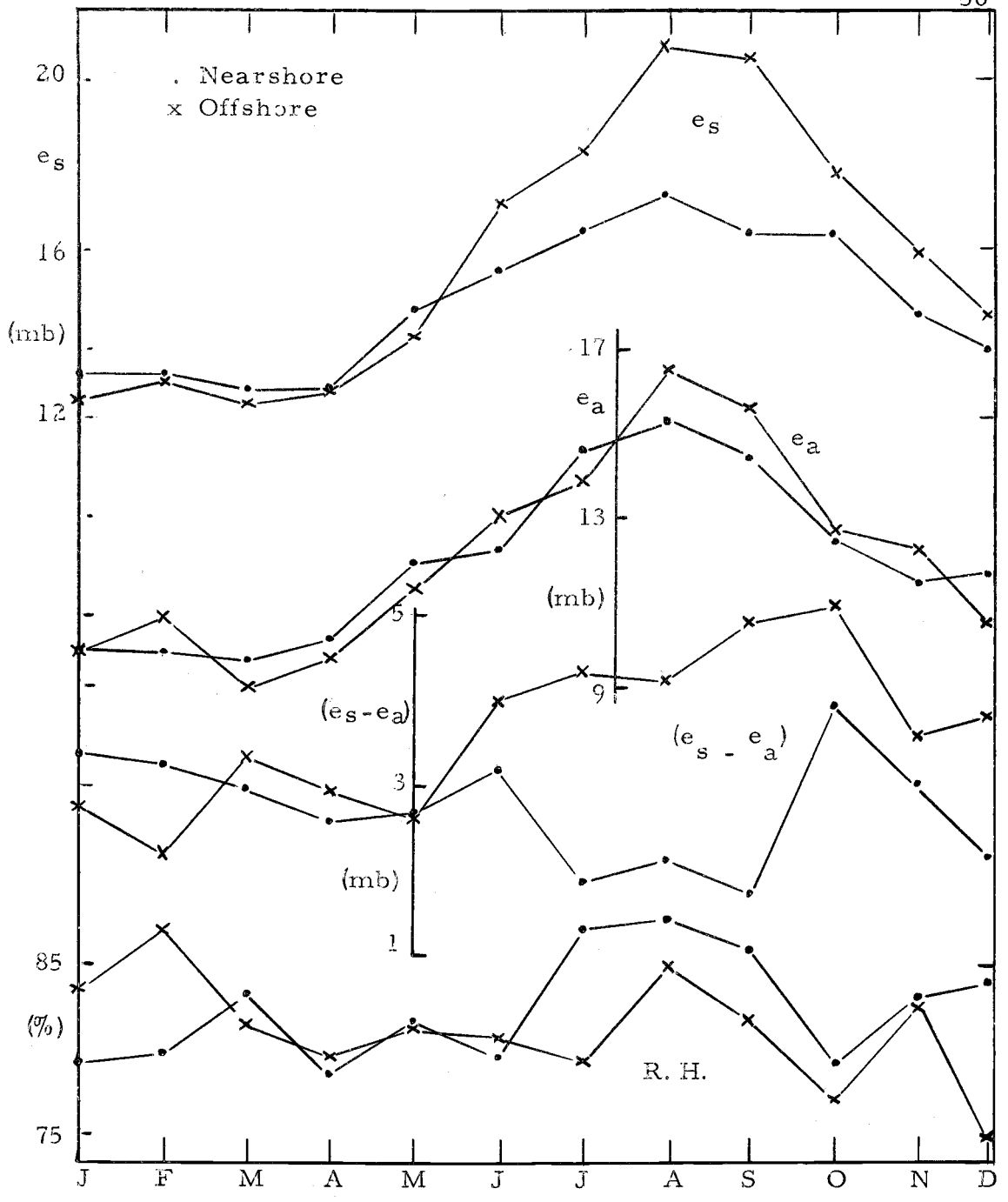

Figure 12. Comparison of nearshore and offshore 11-year means (1952-1962) of: saturation vapor pressure, e_s, atmospheric vapor pressure, e_a, e_s-e_a, and relative humidity, R. H.

cooling due to continental effects, may be dismissed. The order of influence is then: meteorological (wind stress causes oceanic divergence), then oceanographic (cool water upwells in the nearshore region), and finally a combination of the two (air moving from warmer regions is cooled by the upwelled sea surface waters).

For the years studied by the author, the monthly mean differences between the sea surface temperatures of the sub-regions reached a maximum of 5 to 7 F^{o} in the summer (Fig. 9). This difference may be interpreted as a negative temperature gradient (positive means a temperature increase shoreward), and it is seen that the net annual gradient in the sub-regions is negative. To properly evaluate the effect of the convergence-divergence processes on the sea temperature gradient, it is necessary to estimate the gradient that would theoretically exist in the Overall Region in the absence of summer divergence (upwelling) and winter convergence. This was done by projecting the trajectories of sea surface isotherms into the Overall Region from the Eastern North Pacific Ocean. Charts of long-term means of sea surface temperature are included in the Climatological and Oceanographic Atlas for Mariners (39). As mentioned previously, the West Wind Drift spits into northward and southward moving branches off the northwest coast of the United States. Hence, in summer months, the gradient off Oregon due to the general

oceanic circulation is positive while it is negative in winter months. Estimated values of this gradient of sea surface temperature in F^{o}/100 nautical miles are given in Table II. In May the positive gradient is highest at 0.5 F^{o}/100 nautical miles. The negative gradient is highest in November, -1.3 F^{o}/100 nautical miles. The annual mean is about -.07 F^{o}/100 nautical miles. The annual mean gradient between the two sub-regions was determined to be about -1.6 F^{o}/100 nautical miles. Hence, the summer upwelling situation is dominant in affecting the coastal temperature gradient over the period of a year. This does not mean that the upwelling or divergence in summer is necessarily stronger than the winter convergence along the coast since the upwelling introduces gradients which are related to the vertical temperature structure in the nearshore system while the convergence process affects only the weaker horizontal temperature gradients.

Also included in Table II are monthly values of air temperature gradients normal to the Oregon coast which are due only to the general atmospheric flow. They were projected in a manner similar to that used in estimating sea temperature gradients related only to the general oceanic flow. The annual net gradient of air temperature obtained from the Atlas (39) is approximately -0.5 F^{o}/100 nautical miles. The net annual gradient between the sub-regions was determined to be about -0.4 F^{o}/100 nautical miles. These figures indicate that

Table II. Temperature gradients (F^{o}/100 nautical miles) normal to the coast of Oregon (positive if increasing shoreward). 1. Sea surface temperature in the absence of coastal effects deduced from oceanic gradients offshore (adapted from U.S. Department of Commerce (39)) 2. sea surface temperature deduced from sub-region data analyses, 3. air temperature in the absence of coastal effects deduced from offshore atmospheric gradients (adapted from U.S. Department of Commerce (39)), 4. air temperature deduced from sub-region data analyses.

	Jan	Feb	Mar	Apr	May	Jun	Jul	Aug	Sep	Oct	Nov	Dec
1.	-0.2	-0.2	0.2	0.3	0.5	0.4	0.3	0.3	-0.2	-0.4	-1.3	-0.4
2.	1.4	0.4	0.5	0.2	1.4	-2.5	-2.8	-5.2	-6.9	-2.2	-2.1	-1.2
(2)-(1)	1.6	0.6	0.3	-0.1	0.9	-2.9	-3.1	-5.5	-6.7	-1.8	-0.8	-0.8
3.	-1.9	1.1	0	0	0.7	0.1	0	0	-1.1	-1.1	-1.7	-2.5
4.	1.0	-0.1	0.7	1.8	1.5	-1.5	-1.1	-3.1	-3.5	-1.5	-0.7	1.5
(4)-(3)	2.9	-1.2	0.7	1.8	0.8	-1.6	-1.1	-3.1	-2.4	0.4	1.0	4.0

there is little net effect on the air temperature gradient and, therefore, on the air temperature from the coastal processes. Considered seasonally, however, it is seen that these processes are effective in cooling the atmosphere in the nearshore region in the summer and warming it in the winter. It should be pointed out that any winter or summer changes in air temperatures in the coastal region due to an offshore flow of air, affected by continental processes, would be opposite to those observed. In winter, for example, an offshore flow from the continent would be more likely to cause lower air temperatures near the coast because of continental cooling processes in winter months.

As noted in the previous section, the temperature cycles (Fig. 9) show a definite double minimum in winter in the offshore region. This feature also appears in the T_a and T_w cycles from the Overall Region (Fig. 5). In all cases studied, the winter maximum is in February. The number of times that the average values rose from January to February in the offshore region were: for T_a, 6; T_w, 7; and T_s, 9. One explanation would be that the surface waters are undergoing cooling during this season, and it has been shown that this seasonal cooling frequently results in a surface inversion in the vertical temperature structure of the ocean (38, p. 26). At the same time, the surface waters of the offshore region are being moved

northward and toward the shore. If the peak of the onshore convergence should occur during the February cooling period, the cold surface water would be continually removed, leaving a warmer subsurface water exposed.

Another possibility, completely opposite to the one just presented, is that a winter upwelling period or a period of relaxation of the normal convergence pattern may be responsible. Either of these would result from a winter period of northerly winds with enough duration to offset the southerly wind-induced convergence. Why this would occur on a regular basis is not apparent, but there is evidence that periods of mid-winter northerlies do occur along the Oregon coast. Figure 13 contains a plot of 5-day means of sea temperature for the winter of 1962-1963 obtained at Seaside, Oregon (Fig. 1), with 5-day means of hourly wind mileage, directed from either the north or the south. The wind values were obtained from measurements of geostrophic wind at a position 200 miles seaward from Seaside (19). It is seen in Figure 13 that a period of northerlies in January resulted in a strong nearshore cooling, a sequence of events similar to that of summer upwelling.

The relationship between air and sea surface temperatures in the sub-regions is of considerable interest. In both sub-regions, during winter months, the sea surface temperature is higher than the

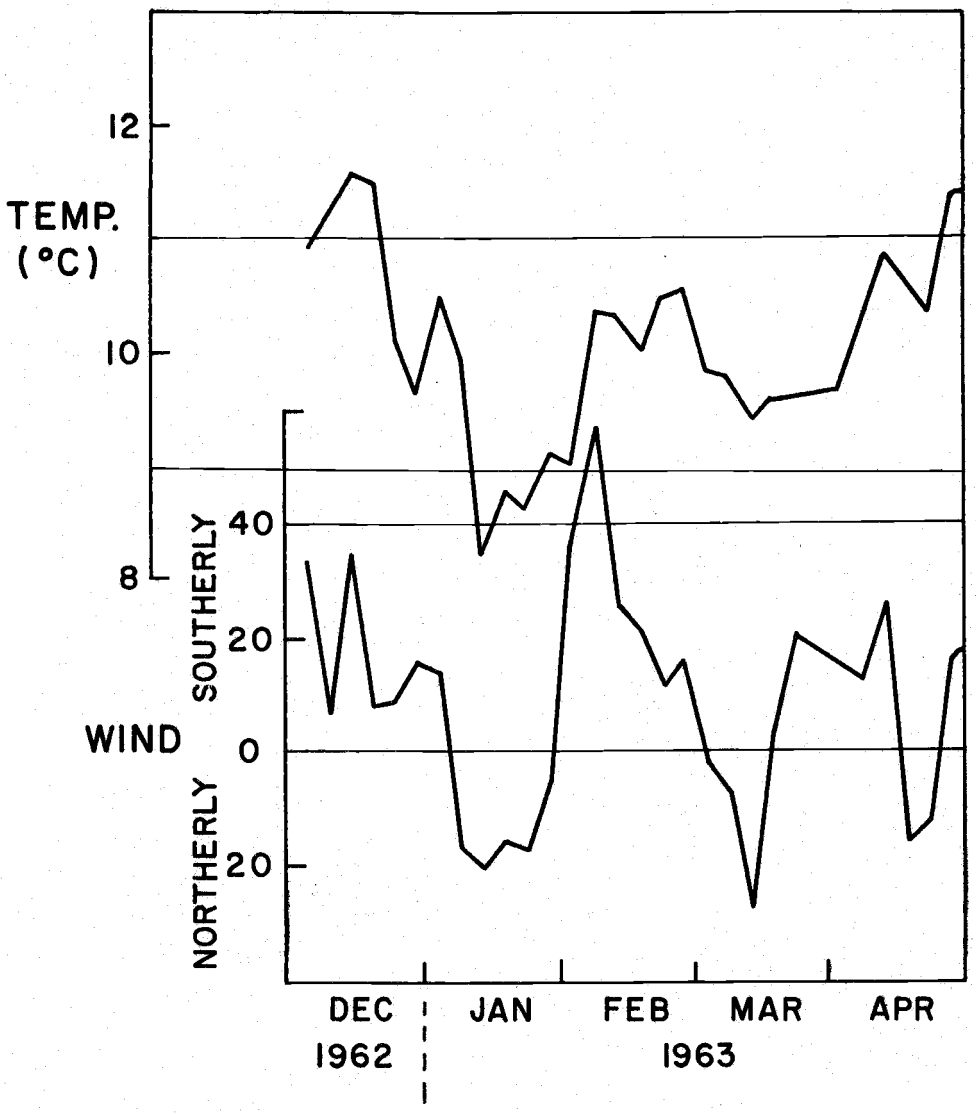

Figure 13. Sea temperature (5 day means) at Seaside, Oregon, and geostrophic wind speeds (5 day means) measured once daily 200 N. miles seaward of Seaside, Oregon.

air temperature. In the summer, however, the nearshore sea surface temperatures fall below the air temperature values while the offshore sea surface remains generally warmer than the air. In 10 of the 11 years studied, the average August sea surface temperature was higher than the air temperature in the offshore region. It was noted that the summer sea surface temperature means were lower than the air temperature means in the Overall Region. This indicates that the summer T_s higher than T_a relationship holds only for the region immediately seaward of the upwelling region.

Two possible explanations of the above exist. The sea surface temperature may be anomalously warmer in the offshore sub-region adjacent to the upwelling. Or, the air flowing over the offshore sub-region may come from the nearshore region and would then be cooled by the upwelled waters. There is evidence that both processes occur. It is shown in Figure 3 that a band of warm water, in the form of a series of pools, does exist seaward of the upwelling region. This feature is attributed to the effluent of the Columbia River, which reaches a maximum in summer (41), and may be assumed to be a regular summer feature. Also, as mentioned previously, an offshore wind flow may occur occasionally during the summer months. With either a wind flow from the northeast or from the northwest, the oceanographic conditions are such as to adequately explain the air-sea

temperature relationship in the offshore region.

The general pattern of the annual variation of mean cloud cover (Figs. 7 and 10) is similar for the Overall Region and the two subregions. As outlined previously, a high pressure area over the North Pacific adjacent to the regions being studied represents the normal summer situation. The cloud cover along the coast of Oregon, however, is also influenced by the summer low pressure area in southern California. Charts 58, 66, 78, 86, 94, and 106 of the Climatological and Oceanographic Atlas for Mariners, Volume II (39), not shown in this thesis, are charts of the mean sea level atmospheric pressure pattern. By May, when the offshore high pressure area is beginning to affect the regions of this study, the California low pressure area is already strongly developed. In August, September, and October, however, before the storm tracks move down to the coasts of Washington and Oregon, the California low pressure area is filling and the region of this study undergoes its period of least cloud cover. During the winter months, storms associated with the Gulf of Alaska low pressure area bring extensive cloudiness to the Pacific Northwest of the United States, despite the formation of a winter high pressure area over the mid-western States.

The seasonal wind pattern (Fig. 10) may also be explained from the seasonal changes in the atmospheric pressure systems. Both

sub-regions are strongly influenced by high winds associated with winter storms which move in from the west and southwest (39). Moreover, the strong summer development of the California low pressure area and the occasional excursion inland of the offshore high pressure region produce frequent northeasterly winds which affect the offshore sub-region sufficiently to cause a summer maximum of wind speed. The nearshore region, somewhat protected by being in the lee of the coastal landmass, has a lower summer peak in July. The September peak in the nearshore region is more difficult to explain. The September mean was computed from monthly averages from 5 years for the nearshore region and from 6 years for the offshore region; but in only 3 years were there both nearshore and offshore data sets where the number of observations exceeded 10. In these 3 years, the average wind speeds (in knots) for the nearshore region (18.6, 22.0, 17.2) and the offshore region (13.5, 22.5, 18.1) were not significantly different over both sub-regions. It is concluded, therefore, that the difference between the September peaks of the nearshore and offshore wind speed means is due to a data bias. It is clear, however, that some of the highest monthly means of wind speed occur in September. The reason for this is not clear, but the fact that the long term means of monthly wind speed at Astoria (Table III) reach a minimum in September suggests high coastal values are due to offshore rather

than onshore air flows. This is in agreement with the predominant direction recorded at Astoria in September (SE, see Table III) but is not a completely satisfactory explanation.

Table III. Long term monthly means of surface wind direction and speed at Astoria, Oregon (Fig. 1).

January	E	8.6 mph	July	NW	8.5 mph
February	ESE	8.7 mph	August	NW	7.7 mph
March	SE	8.6 mph	September	SE	7.2 mph
April	WNW	8.4 mph	October	SE	7.6 mph
May	NW	8.1 mph	November	SE	8.6 mph
June	NW	8.1 mph	December	ESE	8.7 mph

Climatic variables dependent upon the moisture in the air are shown in Figure 12. The nearshore and offshore saturation vapor pressure patterns are directly related to the sea surface temperatures. Hence, the upwelling season is reflected by the lower e_s values in the nearshore region. It is noted that the atmospheric vapor pressure, which depends upon the air temperature and the moisture content of the air, was also generally lower in the nearshore region than in the offshore region in the upwelling period. In the period July to October, the relative humidity in the nearshore region was generally slightly higher (Fig. 12) while the air temperature was lower than in the offshore region. However, in Figure 9 it is seen that the mean T_w values were lower in the nearshore region in summer so that the low e_a values are due to both the low air temperatures and a

lower moisture content.

From the heat and mass transfer standpoint, the most important moisture relationship is that of $(e_s - e_a)$ because it represents the vapor pressure gradient upward from the sea surface, a factor of importance in evaporation considerations. In Figure 12 it is seen that in the summer period, July to September, inclusive, nearshore values of $(e_s - e_a)$ are not only much lower than those in the offshore region, but they are also lower than the winter values in both regions. This is due mostly to the much greater cooling effect of upwelling on the sea surface than on the overlying air. Although it does not appear in the monthly means, it is certain that there are frequent periods in the summer when the sea will be cooled enough that e_s values will fall below those of e_a, in the overlying air. On these occasions, fog may occur (21).

HEAT EXCHANGE ANALYSIS

Techniques for Determining the Heat Budget

Introduction

Oceanographers, meteorologists, hydrologists, engineers, and climatologists have had frequent occasion to apply similar techniques to studies of heat exchange. In many cases, they borrow from each other and modify techniques developed for use in some other field of study.

It is indicative of the importance given to oceanic heat exchange processes that such notable scientists as H. U. Sverdrup, G. Wust, A. Defant, F. Nansen, B. Helland-Hansen, W. C. Jacobs, and H. Mosby have applied themselves to its various problems. Indeed, much of the early work done by these men and others remains today as the basis for heat budget studies.

The study of the heat budget of a body of water is an application of the Law of Conservation of Energy. Consider a volume of water (Fig. 14) with its upper surface in contact with the atmosphere, with its lower surface in contact with a solid (e. g. the floor of the sea), and with its sides in contact with a water medium. The various components of heat exchange between this volume and its surroundings are classified by their direction. Components that enter and leave

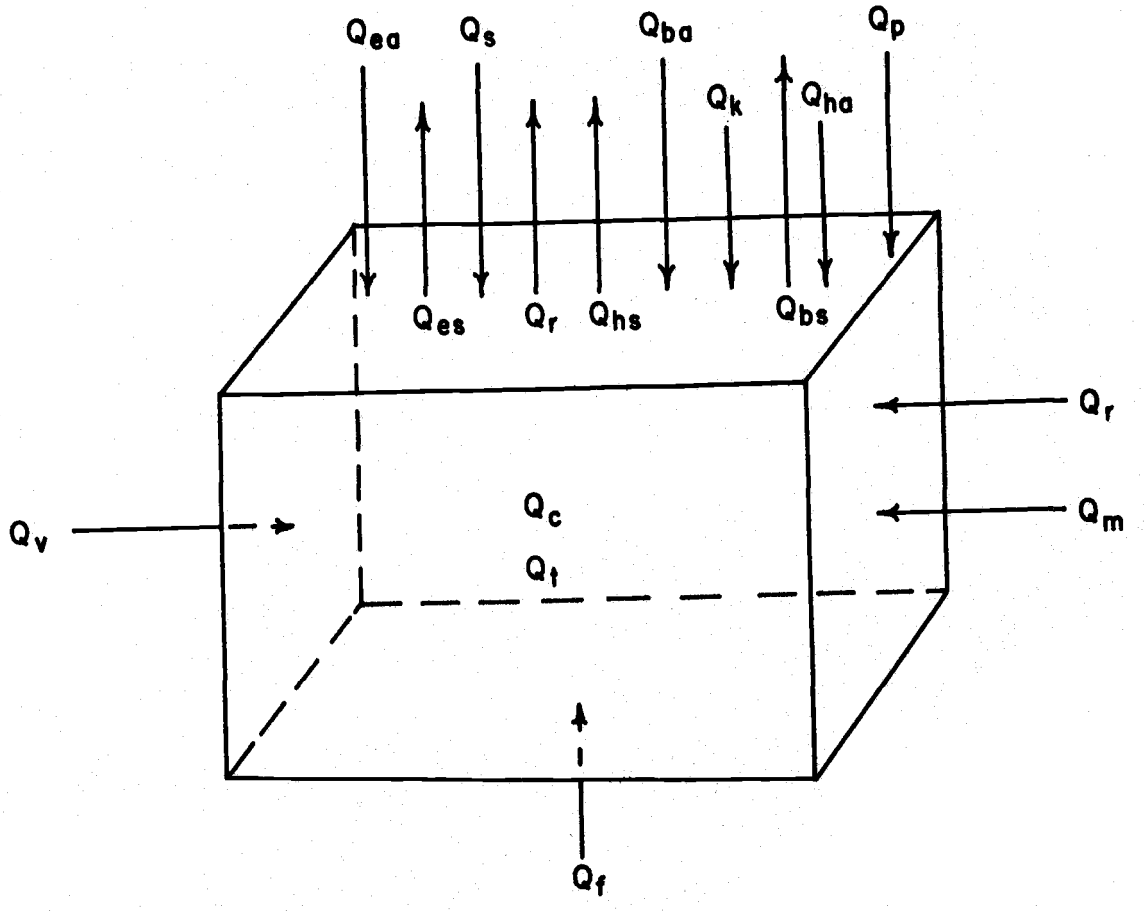

Figure 14. Components of heat exchange affecting a volume of sea water (see Appendix for definitions of Q-terms).

the water volume through its upper surface are:

1. Q_s, solar radiation (direct and diffuse)
2. Q_{ba}, long wave radiation from the atmosphere
3. Q_{ha}, conduction from the atmosphere
4. Q_{ea}, latent heat (condensation)
5. Q_p, heat associated with precipitation
6. Q_k, kinetic energy (wind and tide action)
7. Q_{bs}, long wave radiation from the sea
8. Q_r, reflection of solar radiation
9. Q_{es}, latent heat (evaporation)
10. Q_{hs}, conduction to the atmosphere

Components that enter and leave the volume of water through its sides are:

1. Q_v, advection to and from the surrounding water
2. Q_R, eddy diffusion
3. Q_m, molecular diffusion

Only one component affects the volume of water from the lower surface (Q_f, conduction to and from the sea floor). In addition to the above processes, there are heat changes which occur within the volume of water: Q_c, heat released through chemical processes, and Q_t, heat used to change the temperature of the water.

The study of the terms listed above has been extended into such fields as agriculture, biochemistry, civil engineering, micro-meteorology, and limnology (to name a few). In the past few years, several comprehensive reviews of the more pertinent heat budget techniques have been published. Among these are works by Jacobs (15), Budyko (6), Defant (10), Laevastu (20), and the U. S. Geological Survey (42, 43).

Solar Radiation

The amount of solar radiation received by the Earth on a unit area held facing the sun at the outer edge of the atmosphere when the Earth is at its mean distance from the Sun is essentially constant. This "solar constant" is valued at 1. 94 calories per square centimeter per min. (29) (i. e., 1. 94 langleys per min.).

As the sea surface is not always perpendicular to the path of this solar radiation and because of the attenuating and reflecting properties of the atmosphere, the amount of solar radiation reaching the sea surface per unit area varies as to latitude, time of day, time of year, and atmospheric composition.

Kimball (16) and Black (2) have published ocean charts of average incident solar radiation, under conditions of both zero and average cloudiness. Kimball's charts were based upon an average

atmospheric turbidity and the formula

$$Q_s = Q_o (0.29 + 0.71 (1 - c)). \quad (5)$$

Here, Q_o is the value of solar radiation under zero cloudiness. Black found a quadratic relationship between Q_s/Q_a and used the equation

$$Q_s = Q_a (0.803 - 0.340c - 0.458c^2). \quad (6)$$

Here, Q_a is the amount of solar radiation received in the absence of an atmosphere. Both sets of charts were based on sparse information of oceanic cloud cover.

Equations similar to the above have also been developed by Fritz (12) and Laevastu (20). Such equations are useful when distributions of solar radiation are required over large areas or in small regions where measurements have not been made. It is more desirable, however, to either measure solar radiation at the study site or to make corrections for latitude and cloud cover of data obtained from a nearby station. In the present study, solar radiation data obtained with a pyrheliometer at the Astoria (Fig. 1) U.S. Weather Bureau station were corrected and used as the mean total solar radiation incident at the sea surface. This data is available from January 1953 to present (40) in the form of monthly means of total daily solar radiation incident at the surface. In studying the heat budget of the Overall

Region, it was found that no correction for latitude was necessary because the latitude upon which the radiation is an average value for a certain region is slightly northward of the geographically mean latitude of that region. From List's (29) charts of global radiation, Astoria's latitude (46.09 N) is very close to the latitude of average Q_a for the region 40 N to 50 N. Equation 5 was used to correct for the difference in cloud cover between Astoria and the mean for the Overall Region.

In examining the heat budget of the sub-regions, it was necessary to correct for a difference in latitude. The latitude at which Q_a is the average for the latitudinal distance covered by the sub-regions (Fig. 1) is approximately 44.5 N from List's charts. Assuming that the composition of the atmosphere, in the absence of clouds, is the same over Astoria as it is over the sub-regions, values of Q_o for the sub-regions were computed using the equation

$$Q_o(\text{s. r.}) - Q_o(\text{Ast.}) = \frac{dQ_o}{d\theta}\, d\theta \qquad (7)$$

where (s. r.) and (Ast.) denote sub-region and Astoria values, respectively, and $dQ_o/d\theta$ is obtained over the 5-degree interval 42.5 N to 47.5 N from Black's charts of Q_o (2). θ is the angle of latitude. That is

$$Q_o(\text{s. r.}) = Q_o(\text{Ast.}) + \left[\frac{Q_o\,(42.5^{\circ}\text{N}) - Q_o\,(47.5^{\circ}\text{N})}{5^{\circ}}\right](1.6^{\circ}) \qquad (8)$$

Values of Q_o (Ast.) were obtained by applying equation 5 to the pyrheliometric data from Astoria. Values of Q_s for each of the sub-regions were obtained by using equation 8 with cloud cover values shown in Figure 10 (using monthly means obtained from averages of at least 4 observations).

Some of the solar radiation incident at the sea surface is reflected away and must be computed as a component of the heat budget. The percent of incident radiation that is reflected away is called the albedo and varies as to the time of day, time of year, latitude, state of the sea surface (rough or smooth), and the turbidity of the atmosphere. The latter condition determines the amount of direct and diffuse incident radiation and has a bearing on the angles at which portions of the incident radiation strike the sea surface. The time of day and time of year also influence the angle at which the radiation is incident. The state of the sea determines the effective angle at which the sea surface is inclined to the radiation. The albedo at any particular time and place is therefore dependent upon atmospheric and oceanic conditions at that time and place. However, the total possible range of daily mean values in mid-latitudes over the period of a year varies approximately from 4 to 20 percent, and the range of daily means over the period of one month varies approximately 0.5 - 2.0 percentiles at a given mid-latitude. For the range of accuracies expected in this study, it was pointless to attempt to evaluate the actual roughness parameters for the sea

surface or the actual atmospheric turbidity for each month over the 11 years. Instead, monthly estimates of turbidity and roughness were used with monthly statistics of solar altitude to determine the monthly albedos. Burt (7) prepared a table of albedos related to solar elevation, cloud cover and wind speed. This table was used by Burt to determine monthly means of albedo for the Snake River (Idaho) reservoir region (8). In these studies, as well as in the study of albedo at Lake Hefner (41), it is shown that the solar angle is the governing consideration in the determination of albedo, over a wide range of wind speeds and cloud covers. Hence, the albedos for this study were estimated directly from those computed for the Snake River area (8) and for a proposed reservoir near Medford, Oregon (24), using Burt's technique. Table IV contains monthly averages of albedo for both of these studies. Using the mean of these albedos as the basis, the albedos for the study regions were estimated by applying a slightly larger roughness factor (see Table II, and (7)). It is seen (Table IV) that this change in roughness factor affected the winter values somewhat but had little effect in changing the summer values.

Long Wave Radiation

Approximately 99 percent of the solar radiation received by the Earth is contained between the spectral limits of 0.15 and 4.0

Table IV. Monthly mean values of albedo for: 1. Snake River, Idaho, region, 2. Medford, Oregon, region, and 3. Sub-regions of this study.

	Snake River	Medford	Sub-regions
January	12	9	13
February	9	8	10
March	7	8	8
April	6	7	7
May	6	6	6
June	6	6	5.5
July	6	5	6
August	6	6	7
September	6	8	8
October	8	8	10
November	11	9	13
December	14	9	17

microns (13, p. 75). Solar radiation absorbed by the Earth and its atmosphere is balanced by an outgoing flux of "terrestial" radiation contained within the spectral limits of 4.0 and 80.0 microns (13). This is frequently termed "long wave" radiation or "back" radiation.

Long wave radiation is emitted by all terrestial and atmospheric absorbers; there is considerable exchange of such radiation between the sea and the atmosphere. The atmosphere absorbs "strongly" in the wave lengths of radiation emitted by the sea surface, whereas it absorbs "weakly" in the wave lengths of solar radiation. Thus, a high percentage of solar radiation which is not scattered or reflected in the atmosphere reaches the sea, but a very small percentage of the radiation emitted by the sea passes through the atmosphere. Also, a

large percentage of the radiation subsequently re-radiated by the atmosphere is returned to the sea. Thus, the sea receives a much larger quantity of radiation than it would if there were no atmosphere.

There is normally a net loss of long wave radiation by the sea, termed the "effective" back radiation. Although long wave radiation may be measured directly with radiometers, very few of these devices are in use and practically none are being used at marine stations. The effective back radiation is therefore estimated by individual considerations of incoming sky radiation and outgoing sea radiation. The latter is normally estimated by considering the sea to be very nearly a black body (i. e. absorptivity is 1) and using the Stefan-Boltzman relation (13, p. 82)

$$Q_{bs} = 0.817 \times 10^{-10} K_s^4 \text{ ly} \qquad (9)$$

where K designates absolute temperature. However, since the sea is not exactly a black body, a coefficient (i. e. an absorptivity less than 1. 0) must be introduced to equation 9. Sverdrup (33) and Watanabe (44) used a coefficient of 0. 94, while Anderson (42), working at Lake Hefner, included reflected long wave radiation from the surface in his determination of the coefficient 0. 97. This coefficient is used in the present study.

Atmospheric long wave radiation is a function of the characteristics of the atmosphere (temperature and vapor pressure) and the amount and height of the clouds. Lonnquist (22) reviewed the empirical techniques available at that time and expressed the effective back radiation for a clear sky as:

$$Q_b = 16.2 - 0.09\ T_s - 0.046\ V + 0.12\ \gamma - 1.3\ H \qquad (10)$$

where γ is the vertical lapse rate of air temperature ($^{\circ}C/km$) and H is a humidity factor (2.0, according to Laevastu (20)). Such an equation must have a cloud cover correction. The two most commonly used equations come from empirical work by Kimball (16).

$$Q_b = Q_{b(clear)}\ [\ 0.29 + 0.71\ (1 - c)]\ \ ly/min \qquad (11)$$

and by Moller (according to Laevastu (20))

$$Q_b = Q_{b(clear)}\ (1 - 0.0765\ c)\ \ ly/min. \qquad (12)$$

Recently, Laevastu (20) recommended the combined use of equations 10 and 12 for estimating values of Q_b.

Anderson (42) separated the two components of long wave radiation by measuring atmospheric radiation with a net radiometer and empirically relating his results to atmospheric properties. His analyses resulted in the equation

$$Q_b = 1.141 \left\{ K_s^4 - K_a^4 \left[(0.74 + 0.025\, ce^{-.0584\, h}) + (0.0049 - 0.00054\, ce^{-.06\, h})\, e_a \right] \right\} 10^{-7} \text{ ly/day} \qquad (13)$$

This equation (13) was used by Tabata (36) in his heat budget analysis at Ocean Weather Station "P" (Fig. 2) and was chosen for use in the present study because all the factors needed for its solution were available and it was the result of a careful climatological study.

Conduction - Convection

When the sea is warmer than the overlying air, heat is conducted from the sea surface to the atmosphere. If the warmed air is convectively unstable, it will rise and be replaced at the sea surface by cooler air which in turn, may be warmed and convected upward. In this process, the sea surface water may become cooled to the extent that it also becomes unstable with respect to its environment. Hence, it is possible for the conduction process to instigate convective cells in both the atmosphere and the sea.

In an opposite situation, air being warmer than the sea, the promotion of stability in both fluids results in a smaller exchange of heat. The conduction process is therefore more apt to remove heat from the sea than to add heat to the sea from the atmosphere. Therefore, the conduction term in the heat budget (Q_h) is set positive when

there is a net exchange of heat from the sea to the atmosphere.

The most frequently used technique for estimating Q_h was devised by Bowen (4). He found that the ratio of heat conducted to heat released by evaporation (Q_h/Q_e) is a direct function of measurable meteorological parameters. This ratio is termed the Bowen Ratio (R) and

$$R = \frac{Q_h}{Q_e} = 0.61 \left(\frac{T_w - T_a}{e_w - e_a} \right) \qquad (14)$$

at an atmospheric pressure of 1013 mb. Sverdrup (32) and Anderson (41) have approached this concept in similar manners and generally confirmed the validity of the Bowen Ratio. Equation 14 was selected for the determination of Q_h values in this study.

Heat Supplied by Precipitation

Jacobs (15) and Drozdov (according to Malkus (23)) have published charts of annual rainfall in oceanic regions of the Northern Hemisphere. A comparison of their values (23, p. 130) shows that Drozdov's values are consistently higher than those of Jacobs in the region of the present study. Drozdov's chart (23, p. 130) indicates an annual precipitation of about 2000 mm. By assuming a uniform rate of fall and using the percent frequency of rainfall in this region (39, chart 2), it is estimated that in January one-ninth of the total

precipitation falls (i. e. about 225 mm) and that in July one-thirteenth of the total falls (i. e. about 155 mm). These estimates are intentionally liberal. Thus, less than 10 mm of precipitation falls per day, on the average. If the precipitation has a temperature which averages 5 F^{o} different from the mean temperature of the upper 1 meter of the ocean (with unit surface area of 1 cm^{2}) upon which it falls, then its addition to this volume will cause a change of heat content of 86 calories (using a specific heat of 0. 935 cals/gm), over the period of one month (in this example, January). This is less than 3 langleys per day, an amount of slight significance when the entire heat budget is being considered. Laevastu (20) has pointed out that only under conditions of frequent hail or snowfall will the Q_p term be important.

Heat Exchange Due to Wind or Tidal Action

The frictional dissipation of wind energy at the sea surface and tidal energy within the sea in shallow regions (over the continental shelf or in estuaries) are not large enough terms to be considered in this heat budget. Sverdrup (33) estimated that wind energy amounted to about one ten-thousandth of the energy from incoming solar radiation. Tidal energy dissipation is greatest in shallow regions. It has been estimated at 1050 langleys/year in the Irish Channel (35, p. 110) and in the Bay of Fundy (20, p. 22). Recently, Blanton (3), working

in Coos Bay, Oregon, measured the dissipation of tidal energy in that estuary. Using his results, the author calculated that the energy received by the water was approximately 660 langleys per year. This is about the same magnitude as the amount of solar radiation received in Oregon per day during summer months. The kinetic energy term is also ignored in the heat budget computations of this thesis.

Latent Heat Processes

The use of heat energy in the evaporation process and the release of heat in the condensation process are the only latent heat processes which occur in the area being studied. Condensation is treated here as negative evaporation.

The evaporation process is one of the most important heat budget terms, yet it is rather poorly understood in oceanic regions. The techniques for estimating or measuring evaporation may be classified as follows.

1. The continuous mixing concept - a mathematically derived technique which assumes that the water vapor at the sea surface is diffused downwind in eddies where continuous mixing takes place. The mathematics of the model require assumptions about the vertical wind profile and a knowledge of diffusion coefficients. These coefficients are not as yet well defined.

2. The mixing length concept - a mathematically derived technique based upon turbulence theory developed by Prandtl and Schmidt (see Anderson, et al, (1)) which assumes an atmospheric model consisting of three layers - laminar, intermediate, and turbulent. Each layer requires a mathematical treatment of the wind profile and assumptions about the diffusion coefficients.

3. Energy budget technique - this generally assumes a simplified heat budget equation, wherein all terms are obtainable except Q_e. This technique has been used in several recent lake and reservoir studies (42, 43, 5).

4. Water budget technique - similar to the energy budget technique except that all the terms of inflow and outflow are measured and inserted in a water budget equation to determine the amount of water evaporated.

5. Dalton's technique - like 1 and 2, this is a mass transfer technique. The equation is basically

$$E = k(e_s - e_a)\, f(V) \tag{15}$$

where E is the depth of water evaporated, k is an empirically determined constant, and f(V) is an empirically determined linear or nonlinear function of wind speed, V.

6. Direct or indirect measurement - direct measurement of evaporation almost necessarily involves the implementation of a total water budget, indirect measurements generally utilize an artificial evaporating surface such as a pan of water, a porous surface or a sample of soil.

In oceanic regions, it is impossible to account for all the terms of even a simplified water budget equation. The distribution and extent of precipitation is very poorly known in oceanic regions and sea level heights are only known accurately near islands. The use of evaporation measuring devices, such as pans (e. g. Wust's 1920 measurements, discussed by Defant (10)), has been quite unsuccessful, partly because it is difficult to duplicate conditions at the air-sea interface and partly because it is difficult to arrange a device which will not spill or permit spray to interfere with the measurements.

The mass transfer techniques which use mathematical models of atmospheric turbulence may ultimately be the best way of approaching the problem. At present, however, there is sufficient uncertainty in regard to the form of the equations involved and the values of the coefficients employed to prevent their use in marine studies. The mass transfer approach of Dalton (1), however, has been frequently employed by both limnologists and oceanographers. One of the least complicated of this type of equation (equation 15) originated

with Sverdrup (34)

$$E = 0.105\ (e_s - e_a)\ V \quad \text{mm/day.} \tag{16}$$

Anderson (42) and Tabata (36) have recently used this equation in their heat budget analyses.

Penman (27) revised Dalton's equation to:

$$E = (e_w - e_a)\ 0.35\ (1 + 9.8 \times 10^{-3}\ V)\ \text{mm/24 hr.} \tag{17}$$

Rohwer's equation (see Laevastu (20, p. 47)) is:

$$E = (0.26 + 0.154\ V)\ (0.98\ e_w - e_a)\ \text{mm/24 hr.} \tag{18}$$

Kohler's equation (see Laevastu (20, p. 47)) is:

$$E = (0.13 + 0.138\ V)\ (e_w - e_a)\ \text{mm/24 hr.} \tag{19}$$

There has been much debate (see, for example, Laevastu (20)) on the relative merits of the various equations presented above. There is much work to be done before the evaporation from the oceans is determined with confidence. For the purposes of this study, the equation of Sverdrup , as used by Tabata (equation 16) was selected for use.

Heat Conducted To or From the Bottom of the Sea

Although very few measurements of heat conduction from the floor of the ocean have been made, it is assumed that it is negligible. Laevastu (20, p. 22) has tabulated a range of values from 50 to 80 langleys per year, evaluated by Helland-Hansen and Bullard.

Heat Released by Chemical Action

Laevastu (20) has estimated the heat released to the ocean by chemical action at 235 langleys per year, assuming that the main process is photosynthesis. This term is also omitted in the present study.

Heat Advected or Diffused

In some regions of the World Ocean, the advection term is of prime importance. For example, the fast flowing eastern boundary currents, such as the Gulf Stream in the North Atlantic and Kuroshio in the North Atlantic, are instrumental in advecting large amounts of heat to northern latitudes. Also, energy may be spread horizontally or vertically by both eddy and molecular diffusion, although the latter is generally ignored in oceanic studies because of the larger magnitude of diffusion due to turbulent eddies.

The main objective of the present study is to compare the climate and surface heat exchanges in an upwelling and a non-upwelling region. It was therefore decided to omit any consideration of advected or diffused heat. By doing this, there is also introduced justification for eliminating the Q_f, and Q_c terms without examining them on their own merits.

Net Heat Exchange

The heat budget equation used in this study reduces to

$$Q_t = Q_s - Q_r - Q_b - Q_h - Q_e \tag{20}$$

where Q_t is taken to be the net heat introduced at the surface of the sea which is converted to internal energy and is used to change the temperature of the sea. When the sea receives a positive net amount of heat energy, Q_t is positive.

Heat Budget Program

To compute the heat budget, it was necessary to apply equations 13, 14, and 15 to all the monthly data averages of T_a, T_w, T_s, V, c, and h which were obtained by averaging monthly sets of ship reports by a special machine language program. With each set of data, the computer was also given the appropriate monthly value of the albedo, r.

Values of e_s and e_a are required for equations 13, 14, and 15. These were computed according to the equations 1 and 4. The e_s versus T curve (see equation 1) was arbitrarily divided into three sections which were linearized for use by the computer. The temperature ranges for these sections are: T less than 7.0°C, T between or equal to 7.0°C and 13°C, and T greater than 13°C. From equation 1, the e_s equations used for the given ranges, in order, are:

$$e_s = \left(\frac{0.461}{L}\right) K_s^2 \, (0.34 + 0.029 \, (K_s - 269)), \tag{21}$$

$$e_s = \left(\frac{0.461}{L}\right) K_s^2 \, (0.68 + 0.05 \, (K_s - 280)), \tag{22}$$

and $$e_s = \left(\frac{0.461}{L}\right) K_s^2 \, (1.0 + 0.065 \, (K_s - 286)); \tag{23}$$

where L is the latent heat of evaporation at temperature K_s.

Equations 21 to 23 were also used (with equation 4) to determine values of e_a, except that K_w was substituted for K_s, and L was computed for K_w.

The latent heat varies with temperature, according to

$$L = 4.185 \, (596 - 0.52 \, T) \tag{24}$$

where L is in calories and T is in C°.

The entire heat budget program is given in form of a flow diagram (Fig. 15). This diagram contains the equations used to

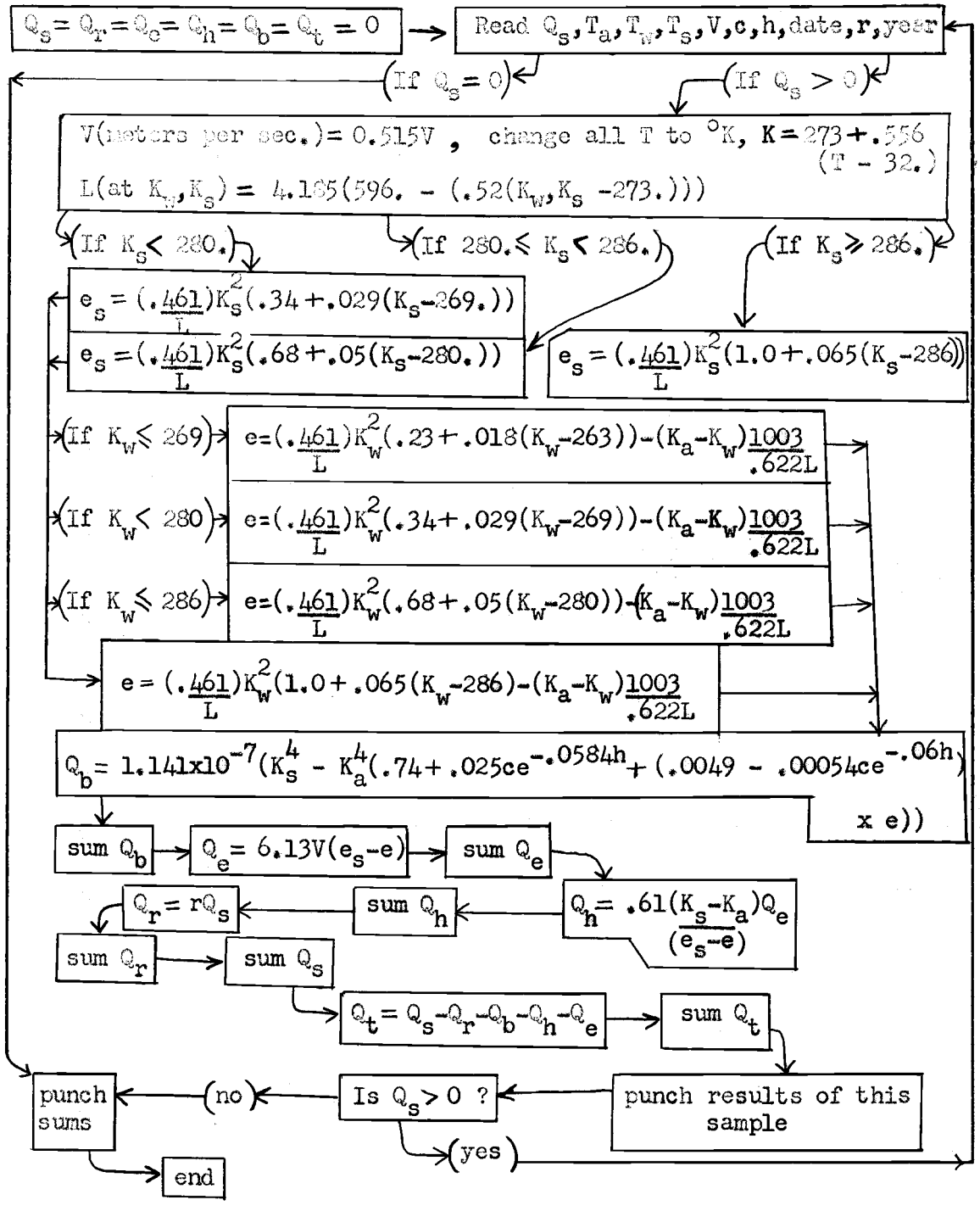

Figure 15. Flow diagram of program for computing heat budget.

compute the heat budget and shows the sequence followed by the computer in using the equations.

THE HEAT BUDGET

Overall Region

Monthly means of total daily solar radiation and reflected solar radiation for the Overall Region are given in Table V. These values were obtained from the Astoria Weather Bureau data as outlined in the previous section. The Astoria station did not record full monthly means of solar radiation until February, 1953. The value shown for January 1953, was obtained by plotting Q_s versus c from the other January data (1954 to 1962) (Fig. 16) and using the monthly cloud cover observed over the last 15 days of that month (10 tenths).

Also contained in Figure 16 is a plot of the July values of solar radiation, corrected for the Overall Region, versus cloud cover. The close correlation evident in both plots confirms that the conversion from Astoria data to Overall Region values of solar radiation, using equation 8, is valid.

Although of small significance, the annual variation of Q_r is interesting in that in 8 of the years studied, there is a small summer minimum. This indicates that the contribution to the Earth's reflected short wave radiation from the Overall Region is frequently not at a maximum when the incoming short wave radiation is at a maximum.

Table V. Monthly averages of total daily incoming (Q_s) and reflected (Q_r) solar radiation in langleys for the Overall Region (Fig. 1).

	Jan	Feb	Mar	Apr	May	Jun	Jul	Aug	Sep	Oct	Nov	Dec
1953												
Q_s	80	246	250	514	472	513	444	420	334	292	115	85
Q_r	10	25	20	36	28	28	27	29	27	29	15	14
1954												
Q_s	87	183	213	547	597	435	417	351	448	323	91	167
Q_r	11	18	17	28	36	24	25	25	36	32	12	28
1955												
Q_s	83	236	279	433	-	524	452	418	278	202	97	86
Q_r	11	24	22	30	-	29	27	29	22	20	13	15
1956												
Q_s	143	137	307	502	555	563	632	619	412	188	95	86
Q_r	19	14	25	35	33	31	38	43	33	19	12	15
1957												
Q_s	211	163	305	368	484	627	654	432	323	202	183	92
Q_r	28	16	24	26	29	35	39	30	26	20	24	16
1958												
Q_s	84	133	388	482	617	419	428	544	363	301	142	93
Q_r	11	13	31	34	37	23	26	38	29	30	18	16
1959												
Q_s	102	144	289	442	566	479	473	450	404	276	176	103
Q_r	13	14	23	31	34	26	28	31	32	28	23	17
1960												
Q_s	103	191	278	356	534	480	402	430	358	198	144	139
Q_r	13	19	22	25	32	26	24	30	29	20	19	24
1961												
Q_s	99	152	311	365	395	703	557	473	476	289	149	84
Q_r	13	15	25	26	24	39	33	33	38	29	19	14
1962												
Q_s	128	256	339	445	532	571	578	440	327	234	116	107
Q_r	17	26	27	31	32	31	35	31	26	23	15	18

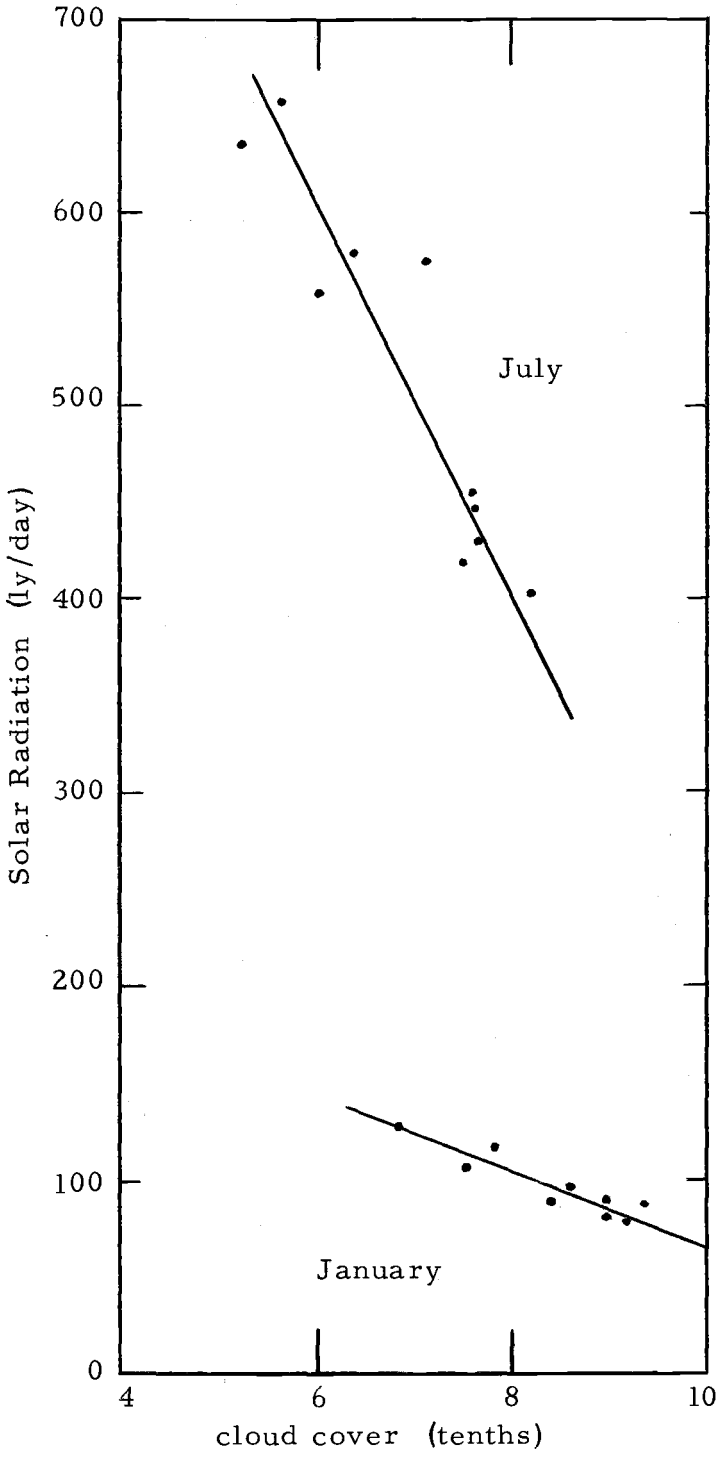

Figure 16. The relationship between solar radiation and tenths of cloud cover for the Overall Region.

Values of Q_b, Q_e, Q_h, and Q_t computed for the Overall Region are shown in Table VI. The annual variation of Q_b shows a weak pattern of lower summer values. This must be attributed to the relatively high $(T_a - T_s)$ values in summer months. The ratio of Q_b/Q_s varies from about 0.5 to a little higher than 1.0 in winter months and as low as 0.1 in summer months. Thus, the radiation budget indicates that there is a strong net input to the sea in summer months and a weaker input or even a weak output from the sea in winter months.

The loss of heat from the sea surface due to evaporation is, over the period of a year, almost double that due to back radiation. It is seen in Table VI that values of Q_e vary considerably both monthly and yearly. As with the pattern of Q_b, summer values of Q_e are frequently less than winter values, although this is not by any means a consistent feature.

The magnitude of the heat loss due to conduction to the atmosphere is generally close to that due to reflection of solar radiation. It is rare that the daily total of Q_h (Table VI) is greater than 70 langleys or that $-Q_h$ (conduction to the sea) is greater than 70 langleys. In the case of conductive losses, values are more consistently lower in summer than in winter while all of the cases of conductive heat gains occur in summer months. This is due to the relationship between air and sea surface temperatures described previously.

Table VI. Monthly mean values of total daily net back radiation (Q_b), latent heat exchange (Q_e), conducted heat (Q_h), and net heat exchange (Q_t) for the Overall Region, in langleys.

	Year: 19--	53	54	55	56	57	58	59	60	61	62
Q_e	Jan	53	139	77	134	233	233	224	206	85	225
	Feb	127	27	114	176	133	62	265	229	320	170
	Mar	119	185	184	56	124	179	161	101	277	193
	Apr	118	159	82	85	52	165	135	204	167	143
	May	62	113	-	116	82	97	150	141	98	208
	Jun	129	175	96	131	62	112	120	123	265	128
	Jul	53	89	69	26	60	128	185	148	18	32
	Aug	23	78	167	82	86	121	221	108	74	41
	Sep	148	209	112	97	79	211	201	200	77	123
	Oct	70	211	87	273	206	269	304	183	266	143
	Nov	294	157	75	95	155	214	237	270	220	267
	Dec	102	195	261	113	219	10	259	187	190	180
Q_b	Jan	43	49	55	127	183	66	68	72	55	86
	Feb	71	77	99	95	67	48	75	77	70	92
	Mar	36	73	87	68	72	99	66	59	69	79
	Apr	88	117	77	80	57	85	82	63	57	72
	May	77	80	--	110	64	65	73	62	42	63
	Jun	64	74	80	72	56	52	46	62	103	69
	Jul	44	51	48	74	70	47	62	49	51	53
	Aug	48	46	77	79	68	86	80	55	65	43
	Sep	81	136	79	63	75	86	78	83	88	69
	Oct	103	137	86	69	83	108	111	67	101	75
	Nov	77	51	65	71	106	87	99	80	83	80
	Dec	51	148	111	49	82	71	89	82	61	81
Q_h	Jan	-5	50	16	83	154	37	54	32	-13	62
	Feb	15	2	16	42	27	-21	55	28	61	34
	Mar	18	52	48	-7	10	8	14	6	62	22
	Apr	12	36	-8	23	-13	2	3	20	10	1
	May	-6	4	-	27	-25	-19	-3	2	-6	22
	Jun	13	17	7	5	-24	-6	-13	-11	-2	-19
	Jul	-19	-20	-25	-45	-38	-29	-5	3	-41	-59
	Aug	-35	-8	7	-50	-15	-16	21	-4	-24	-37
	Sep	9	38	15	-19	-6	13	9	13	-34	-5
	Oct	-31	10	-1	59	24	30	42	19	37	7
	Nov	90	38	24	28	15	36	36	51	28	58
	Dec	-13	25	120	32	30	-10	62	44	26	34

Table VI. Continued

	Year: 19--	53	54	55	56	57	58	59	60	61	62
Q_t	Jan	-21	-162	-76	-220	-387	-263	-257	-220	-41	-261
	Feb	8	59	-17	-190	-80	31	-265	-162	-314	-66
	Mar	57	-114	-62	165	75	71	25	90	-122	18
	Apr	260	207	252	279	246	196	191	44	105	198
	May	311	364	-	269	334	437	312	297	237	207
	Jun	279	145	312	324	498	238	300	280	298	362
	Jul	339	272	333	539	523	256	203	178	496	517
	Aug	355	210	138	435	263	315	97	241	325	364
	Sep	69	29	50	238	149	24	84	33	307	114
	Oct	121	-67	10	-232	-131	-136	-209	-91	-144	-14
	Nov	-361	-167	-80	-111	-117	-213	-219	-276	-201	-304
	Dec	-69	-229	-421	-123	-255	6	-324	-198	-207	-206

Solar radiation and the heat loss due to evaporation have the greatest effect on the annual heat budget. In summer months, there is always a net heat gain by the sea. In winter months, the sea almost always has a net loss of heat to the atmosphere. The sea may gain or lose heat in spring and autumn months; in the years studied, the Overall Region more frequently gained than lost heat during the spring and autumn.

The total net heat transfer for each year is shown in Figure 17 for the Overall Region. The range is considerable, varying from over 42,000 langleys gained by the sea in 1956 to almost 2,000 langleys lost by the sea in 1959. The total heat budget, given for several different intervals in 1956 and 1959, is shown in Figure 18. It is clear that both solar radiation and evaporation were major contributors to the net differences observed. An examination of annual totals shows that in 1956 the sea received 10,335 langleys more (by incident solar radiation) than it did in 1959, while in 1956, the sea lost 32,866 langleys less (due to evaporation) than it did in 1959. This means that the differences in the Q_s and Q_e terms account for over 43,000 langleys or almost the entire difference between the two total heat budgets.

The two years, 1956 and 1959, were examined in detail to determine if any one climatic factor was responsible, to a major degree, for the differences observed in the heat budgets. The climatic

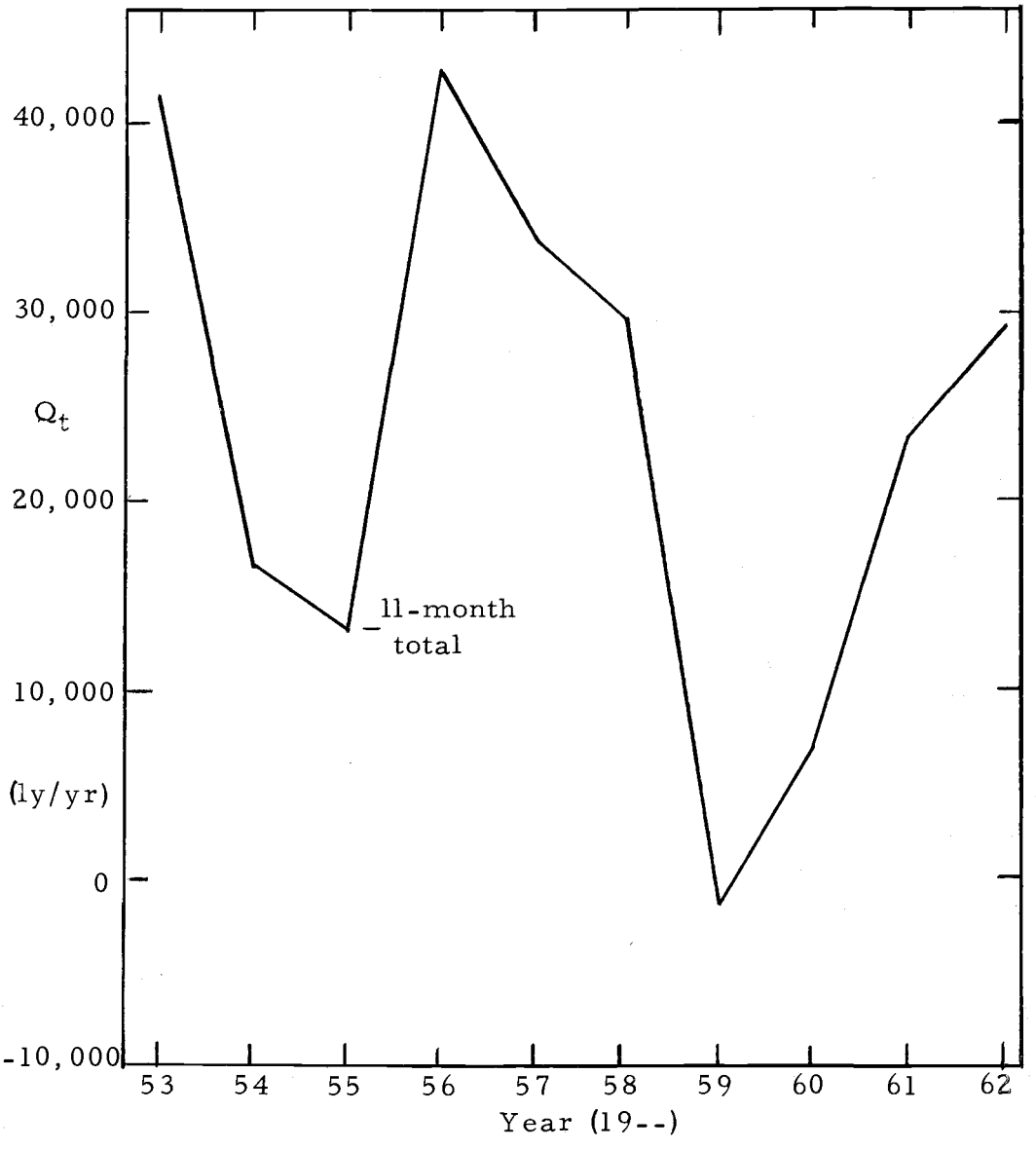

Figure 17. Variation of annual heat exchange (Q_t) from 1953 to 1962 in the Overall Region.

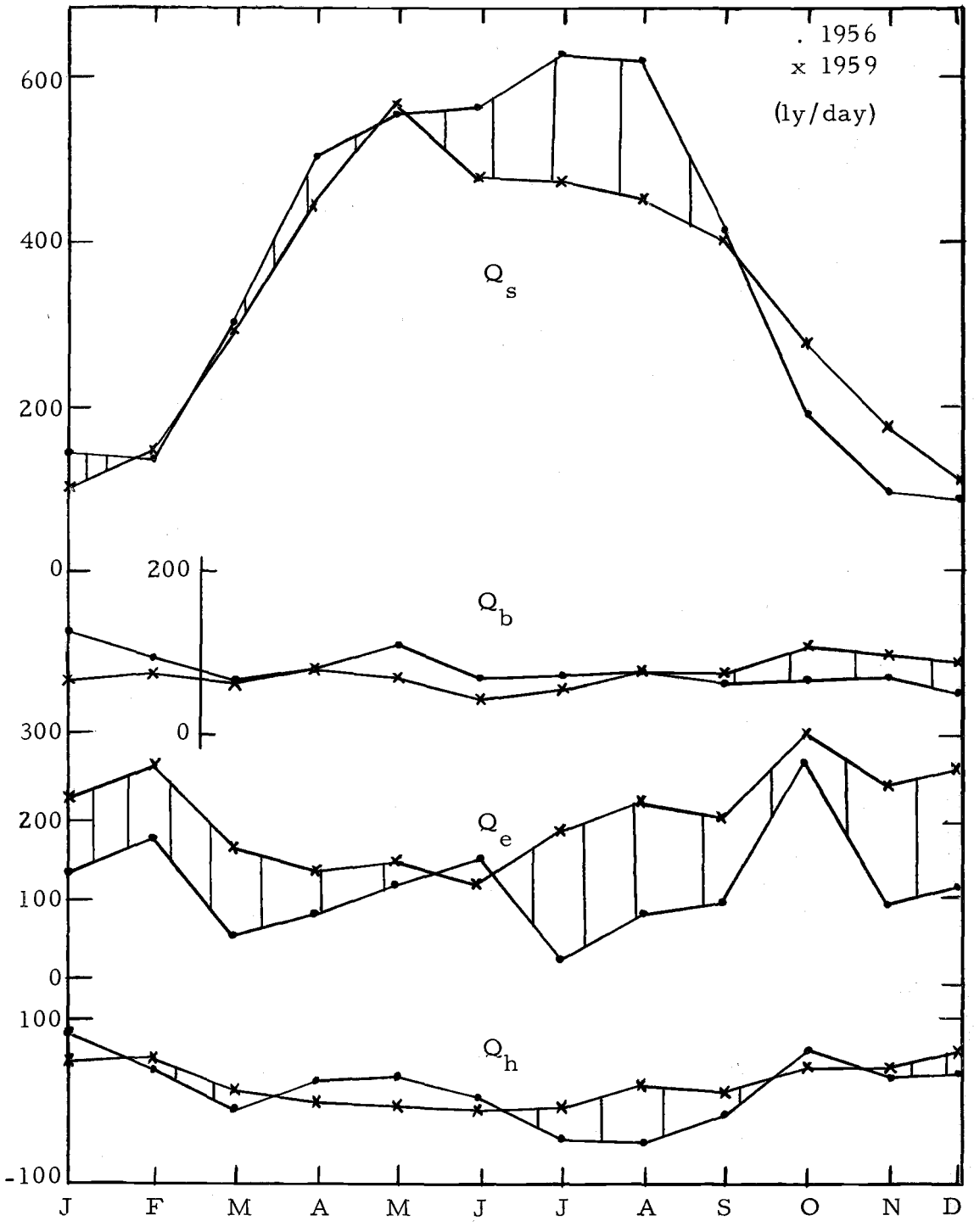

Figure 18. Comparison of monthly means of solar radiation, Q_s, back radiation, Q_b, latent heat, Q_e, and conducted heat, Q_h, in the Overall Region for 1956 and 1959. Hatched areas indicate either greater heat gains in 1956 or greater heat losses in 1959.

factors, used to determine values of Q_s and Q_e, are cloud cover, sea surface temperature, air temperature, wet bulb temperature, and wind speed. The mean monthly values of these parameters, taken from all the years studied, are shown in Figure 19 along with the monthly values from 1956 and 1959. It is seen that the difference in total annual Q_s for the two years may be explained by the differences in the cloud cover values for the critical months of July and August when values of Q_o are high. The 1956 values of c are significantly lower than those of 1959.

The analysis of the change in Q_e is more complex. From equation 16, it is seen that the values of $(e_s - e_a)$ and V are both linearly involved. The differences in monthly values of these factors (Figs. 19 and 20) in the two years being examined indicates that both are substantially higher in 1959. A further examination of the factor $(e_s - e_a)$ reveals that its being higher in 1959 is due mainly to high values of e_s (Fig. 20) which were determined from values of sea surface temperature. Thus it may be concluded that the main climatological difference between the two years having such different heat budgets is that 1959 had less cloud cover in the summer, and higher wind speeds and sea surface temperatures than 1956.

The last of these climatic factors bears further comment. In the period between 1956 and 1959, sea surface temperatures in the

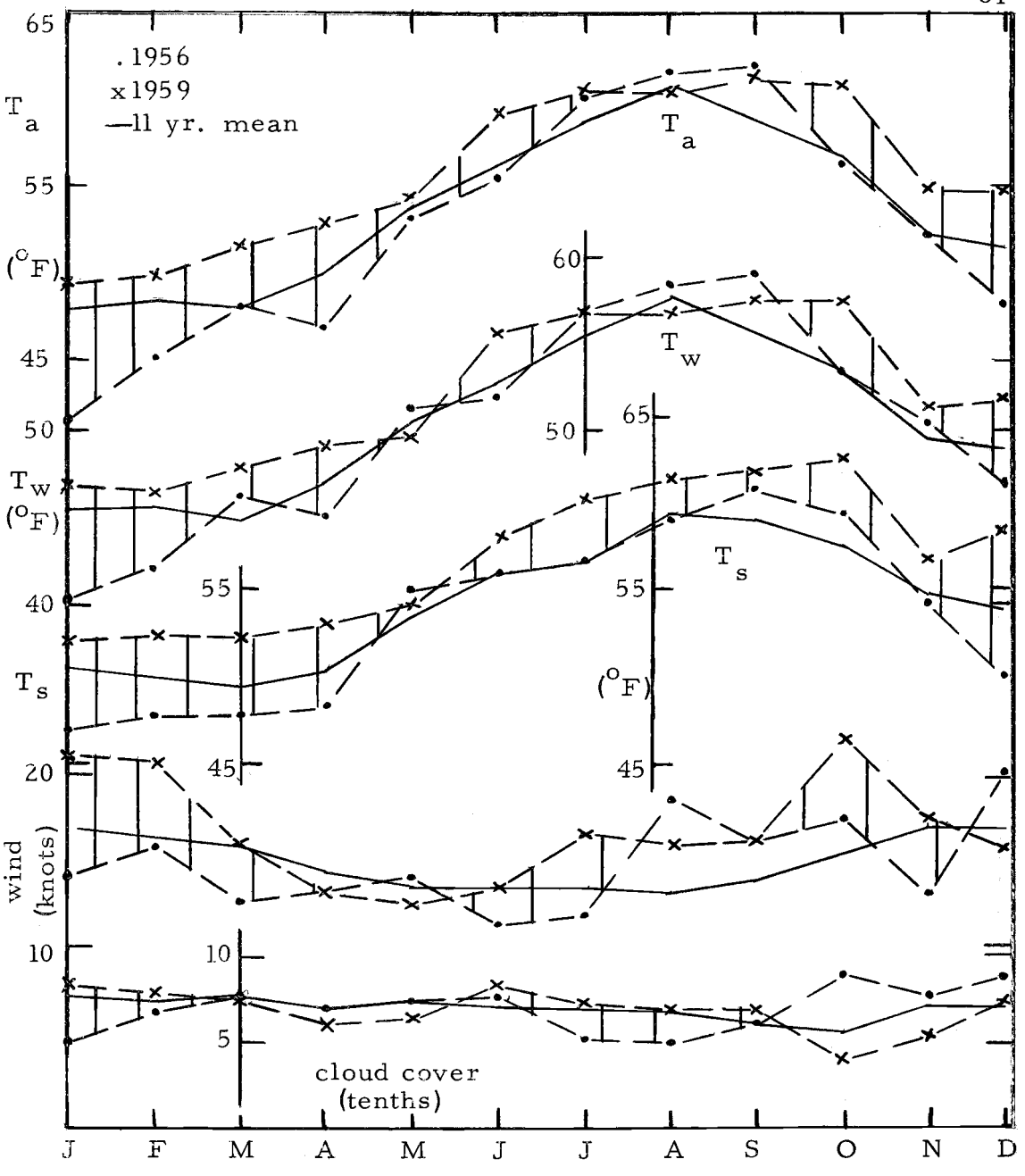

Figure 19. Comparison of monthly means of air temperature, T_a, wet bulb temperature, T_w, sea surface temperature, T_s, wind speed, V, and cloud cover, c in the Overall Region for 1956 and 1959. Hatched areas indicate periods when values were higher in 1959.

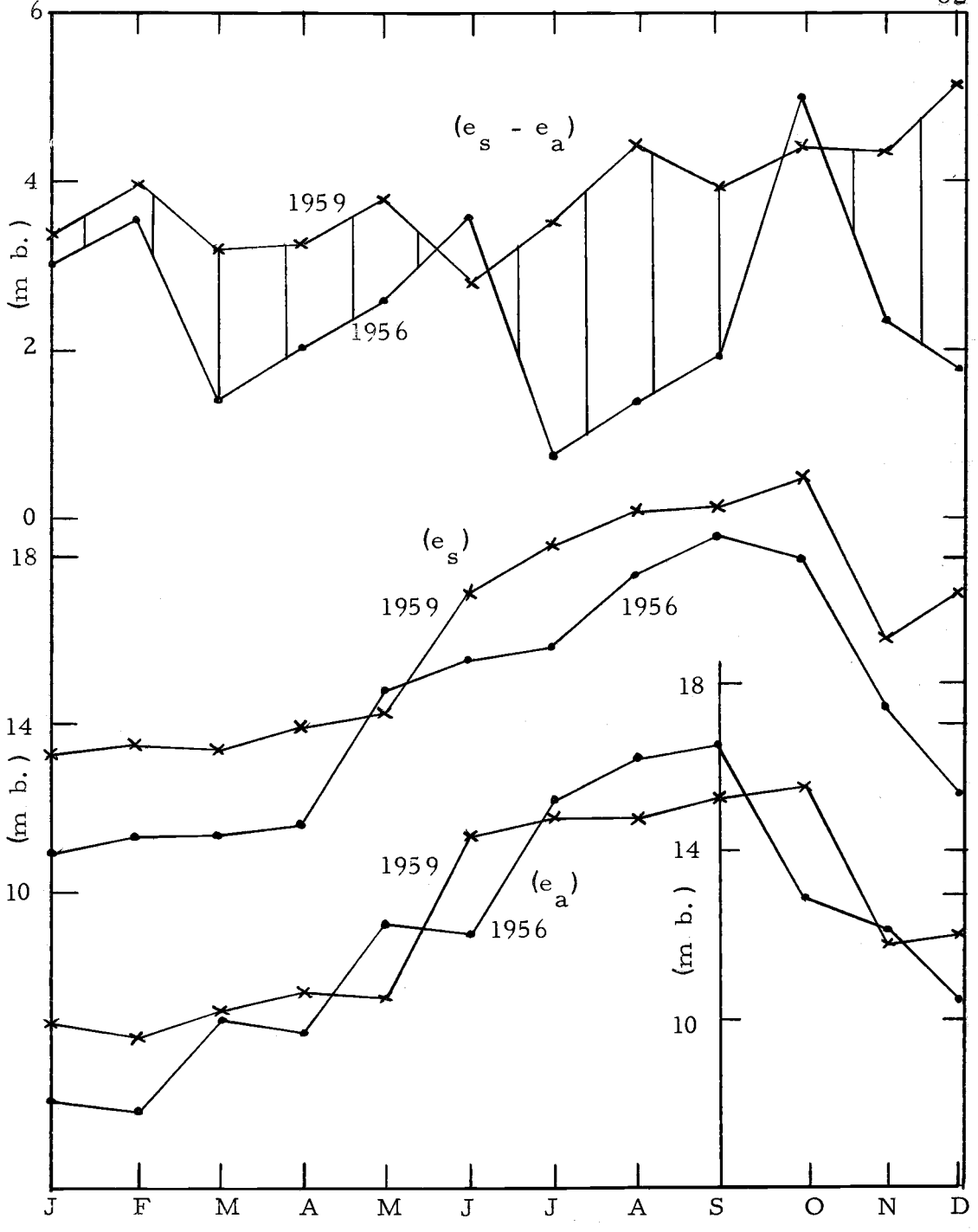

Figure 20. Comparison of monthly means of saturation vapor pressure, e_s, atmospheric vapor pressure, e_a, and $(e_s - e_a)$ in the Overall Region for 1956 and 1959.

northeastern side of the Pacific Ocean were unusually high due to an intrusion of water from the south (37). Although it was found that the peak effect of the intrusion in the Gulf of Alaska was evident in early 1958, it is conceivable that the peak was reached in the Overall Region at a later time.

It has been shown that variations of three climatic factors were mainly responsible for large variations in the annual heat budget. It is now necessary to examine these factors to determine if one or more is consistently responsible for annual fluctuations of net heat exchange. A plot of annual net Q_t versus annual mean sea surface temperature T_s is contained in Figure 21. Included in this figure are values of mean cloud cover for the period May to August, inclusive. There is a definite, but poor, correlation between Q_t and T_s, and the influence of c is also apparent in some cases. However, the relationship is not close enough to imply a technique for estimating annual nets of Q_t based upon values of T_s and c. The analysis of the years 1956 and 1959 has therefore succeeded only in indicating the relative importance of some of the climatic elements on net heat exchange.

A further analysis of net heat exchange was made, based upon the relationship between the evaporation process which occurs in a shallow pan and that which occurs in a deep volume of water. In a pan there is little storage of heat; the bulk of the heat received by the

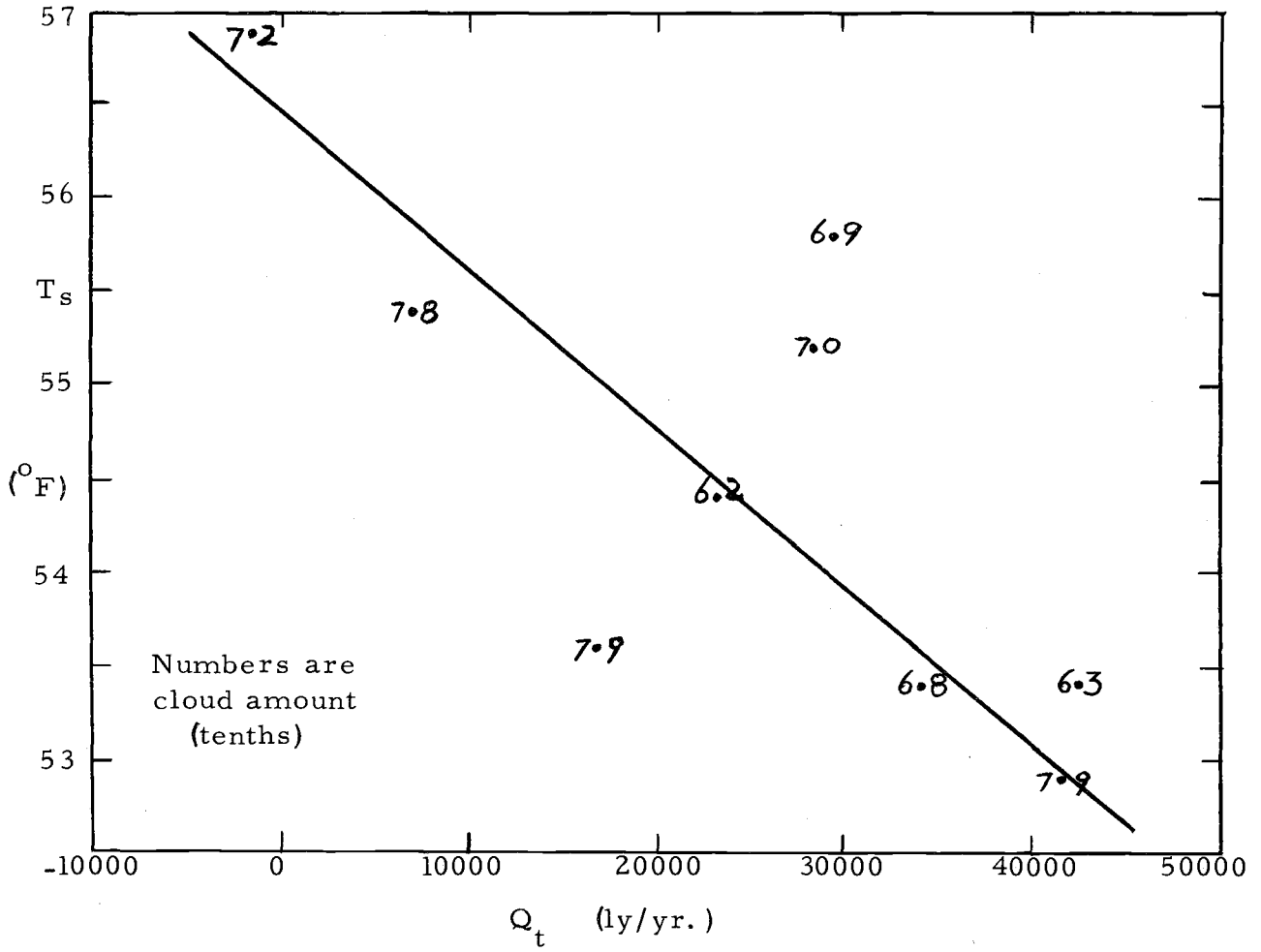

Figure 21. Annual totals of net heat exchange for the Overall Region from 1953 to 1962 plotted against annual means of sea surface temperature, T_s. Values at each point indicate mean cloud cover for the period May to August, inclusive.

water in a pan is near the surface available for use in the conduction and evaporation processes. Thus, it would seem that there is a relationship between the amount of heat stored in a large reservoir or ocean and the difference between the amount of heat lost by evaporation from a shallow pan and the amount of heat actually lost due to evaporation. That is

$$E' - E = f(Q_t) \tag{25}$$

where E' is the depth of water evaporated by a shallow pan under the same climatic conditions that the heat exchange Q_t and the evaporation E occurred.

It has been shown (31, 18) that the evaporation from a shallow Class A U.S. Weather Bureau pan may be estimated by the correlation equation

$$E' = Q_s (a T_a - b) \tag{26}$$

For stations along the west coast of the United States, Lane (18) found that a and b were 2.67 and 51.46, respectively. Thus, inserting equation 26 in equation 25, we obtain

$$Q_s [2.67 T_a - 51.46] - E = f(Q_t) \tag{27}$$

Using monthly means of T_a, Q_s, and Q_e, equation 27 was applied to the data from the Overall Region for the 119 months studied.

Figure 22 contains a plot of $Q_e' - Q_e$ versus Q_t using these data. Clearly, there is a marked correlation, which may be described by the equation

$$Q_e' - Q_e = 0.525\ Q_t - 41.0 \qquad (28)$$

The correlation coefficient in this case is 0.97. Despite this apparently good correlation, it is evident that equation 28 is not an accurate tool for estimating values of Q_t. For example, in Figure 19 it is seen that for a value of $(Q_e' - Q_e)$ equal to 80 langleys per day, values of Q_t ranged from 140 to 320 langleys per day. However, equation 28 provides a technique for generally estimating Q_t in this region when there is insufficient data for a complete heat budget analysis. It is felt that equation 28 would be especially useful for engineering considerations of heat storage in lakes or reservoirs.

Sub-regions

Monthly means of total daily solar radiation were computed for each of the sub-regions from Astoria values, using the technique described in the section on solar radiation. These values are contained in Table VII. Since the north and south boundaries of the sub-regions are at the same latitudes, the difference in Q_s for a particular month is due solely to differences in cloud cover.

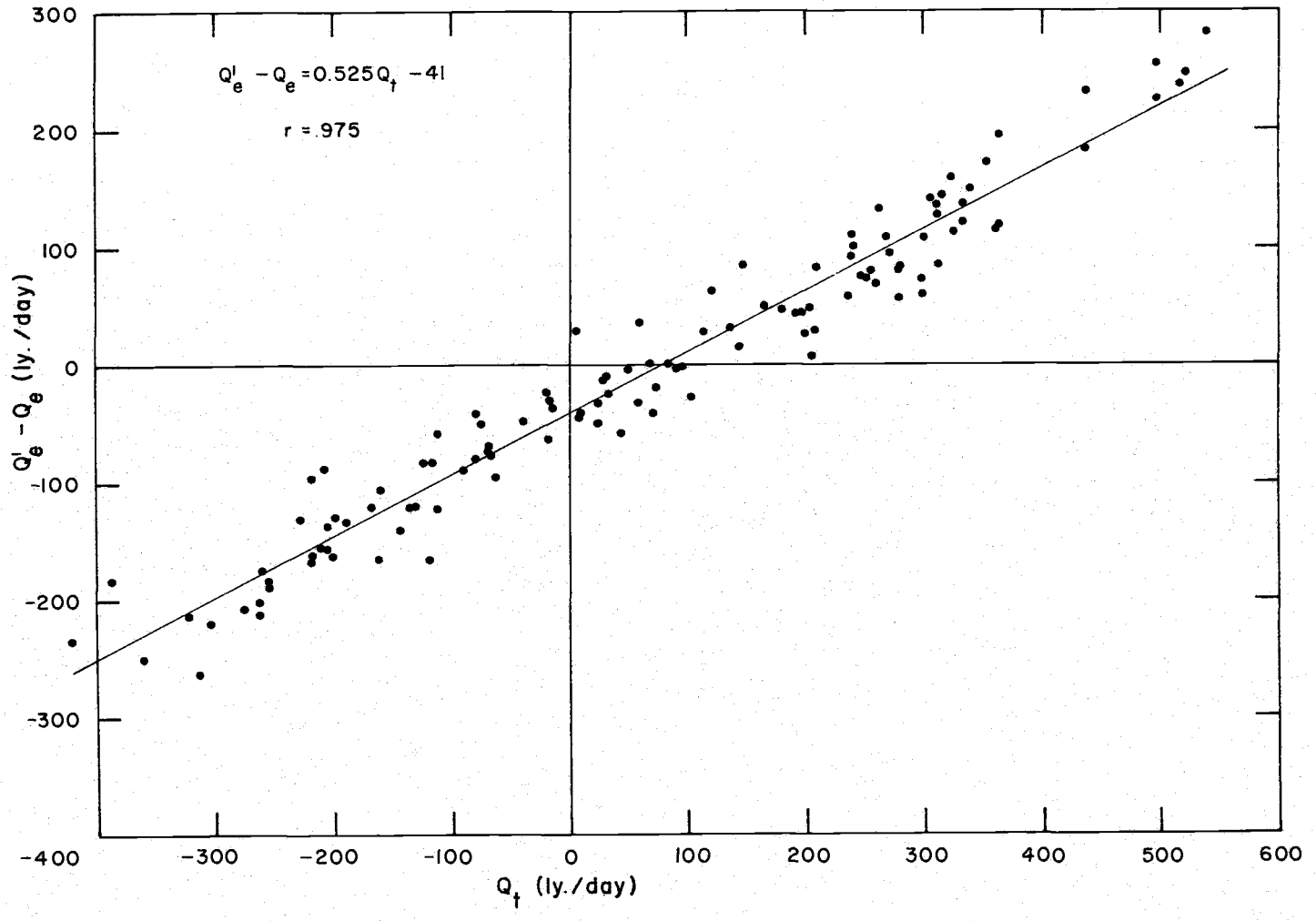

Figure 22. Monthly means of daily net heat exchange in the Overall Region plotted against monthly means of daily values of $(Q'_e - Q_e)$ (See Appendix for Q-term definitions).

Table VII. Monthly means of total daily incident (Q_s) and reflected (Q_r) solar radiation computed for the nearshore and offshore sub-regions (Fig. 1). (Values are averaged for the period 1953-1962, inclusive, and are in langleys)

	Nearshore		Offshore	
	Q_s	Q_r	Q_s	Q_r
Jan	133	17	100	13
Feb	156	16	198	20
Mar	287	23	306	24
Apr	455	32	428	30
May	517	31	528	32
Jun	559	31	525	29
Jul	446	27	455	27
Aug	481	34	383	27
Sep	420	34	380	30
Oct	302	30	270	27
Nov	145	19	145	19
Dec	127	22	95	16

To analyze the average effects of upwelling on the heat budget, averages of the heat budget terms for the years studied were made, month by month. These averages of the individual monthly means are plotted in Figures 23 and 24. The mean values of climatological elements used in the heat exchange equations were determined from monthly averages of at least 4 observations in the case of T_a, T_w, and T_s; and of at least 10 observations in the case of c, h, and V.

There appears to be very little difference in the annual variation of Q_b (Fig. 23) of both regions. It is expected that the nearshore waters, being cooler (Fig. 9), would radiate less energy than the offshore waters in summer and early autumn months. Evidently, the cooling of the overlying atmosphere during upwelling is sufficient to

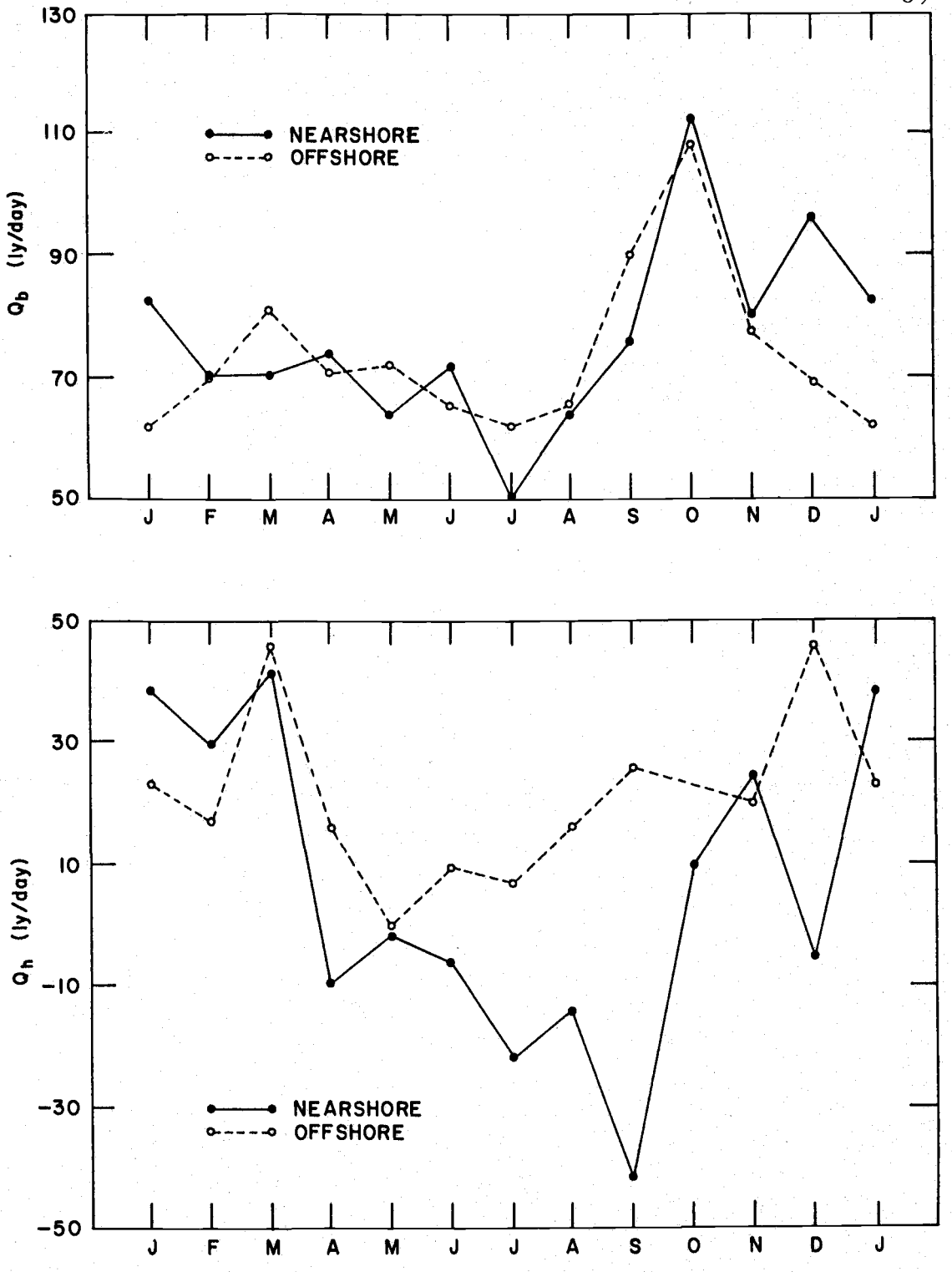

Figure 23. Comparison of nearshore and offshore region values of 10-year (1953 to 1962) means of daily totals of heat loss due to back radiation, Q_b, and conduction, Q_h.

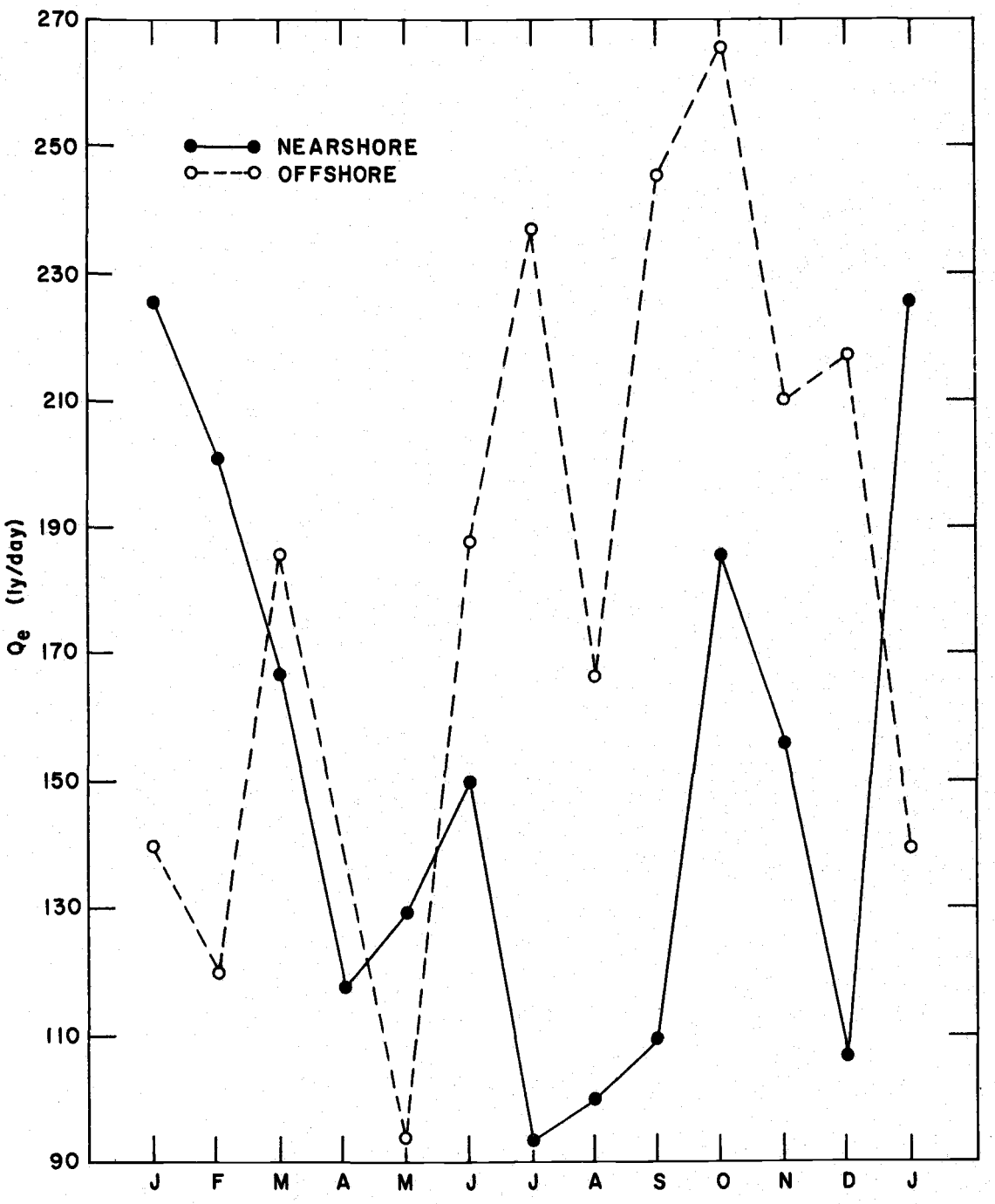

Figure 24. Comparison of nearshore and offshore region values of 10-year (1953 to 1962) means of daily totals of heat loss due to evaporation, Q_e.

reduce incoming long wave radiation and prevent the net back radiation in the nearshore region from falling below that of the offshore region. At the very beginning of the summer upwelling season (i. e. in July) before the atmosphere is consistently modified by the upwelling process, there is a relatively large difference in values of Q_b in the two sub-regions (Fig. 23).

In winter months, the higher nearshore sea surface temperatures result in values of Q_b which are higher nearshore than offshore (Fig. 23).

The effect of upwelling on the conduction term of the heat budget Q_h, is clearly shown in Figure 23. In summer and autumn months, Q_h values in the nearshore region are much lower than those offshore and are negative. That is, in the upwelling region, there is a net conduction of heat to the sea, while in the offshore region during the upwelling season there is a net conduction to the atmosphere.

The important evaporation term (Fig. 24) is also affected by the upwelling process. In the period June to December, inclusive, the nearshore region averages a heat loss due to evaporation of 90 langleys per day less than the offshore region. This also means that the nearshore region evaporates about 2 inches of water a month less than the offshore region. Hence, the processes which cause the climatic differences between these two sub-regions result in a

considerable difference in the amount of water evaporated from them to the atmosphere. This cannot be entirely attributed to upwelling and its effects on the climate. It was shown previously that there is frequently a band of water at the outer edge of the upwelling zone which is warmer than the waters on either side of it. This band of water was attributed to the Columbia River effluent (see section on climate of the sub-regions). The effect of this warmer water in enhancing the difference in E (and Q_e) between the two sub-regions must be considered.

The variations in the discharge of water from the Columbia River is indicated by variations in the discharge of the river at The Dalles, Oregon (Fig. 1). This data is recorded in the Geological Water Supply Papers of the U. S. Department of the Interior (41). Examination of this data for the years 1951 to 1960, inclusive, reveals that the difference between the discharge of the years of highest and lowest total discharge is only 30 percent of the mean total discharges for this 10-year period. Thus, it is not too surprising that there is not a consistent relationship between yearly fluctuations of summer river discharge and values of T_s in the offshore region. An analysis of salinity in the surface waters of the offshore region and the summer discharge from the Columbia River might be the best approach to determining the relative effects of the river water on the temperature

distribution.

The average net heat exchange for the years studied is shown month by month for the sub-regions in Figure 25. In the spring months, the two regions begin to gain heat at about the same rate. By mid-summer, however, the rate of increase of heat begins to decrease in the offshore region. This is attributed to the high surface temperatures due to the Columbia River effluent and high values of cloud cover which reduce the amount of solar radiation incident at the sea surface. The nearshore region, on the other hand, continues to receive a large net heat input through September. The upwelling situation, by reducing sea surface temperatures, is a major factor in this regard. Therefore, while the difference in solar radiation received by the sub-regions is a major factor contributing to the differences in Q_t, especially in August, the largest factor is the difference in heat loss due to the evaporation process (see Figure 24).

If the net heat exchange term were the major factor affecting the change of sea surface temperatures, it would be expected that values of T_s would rise whenever Q_t had positive values, and vice versa. It is shown in Figures 9 and 25 that this situation is true in the offshore region. Sea surface temperature values begin to rise in late April and begin to decrease in September. Net heat exchange in the offshore region also rises to become positive in April and

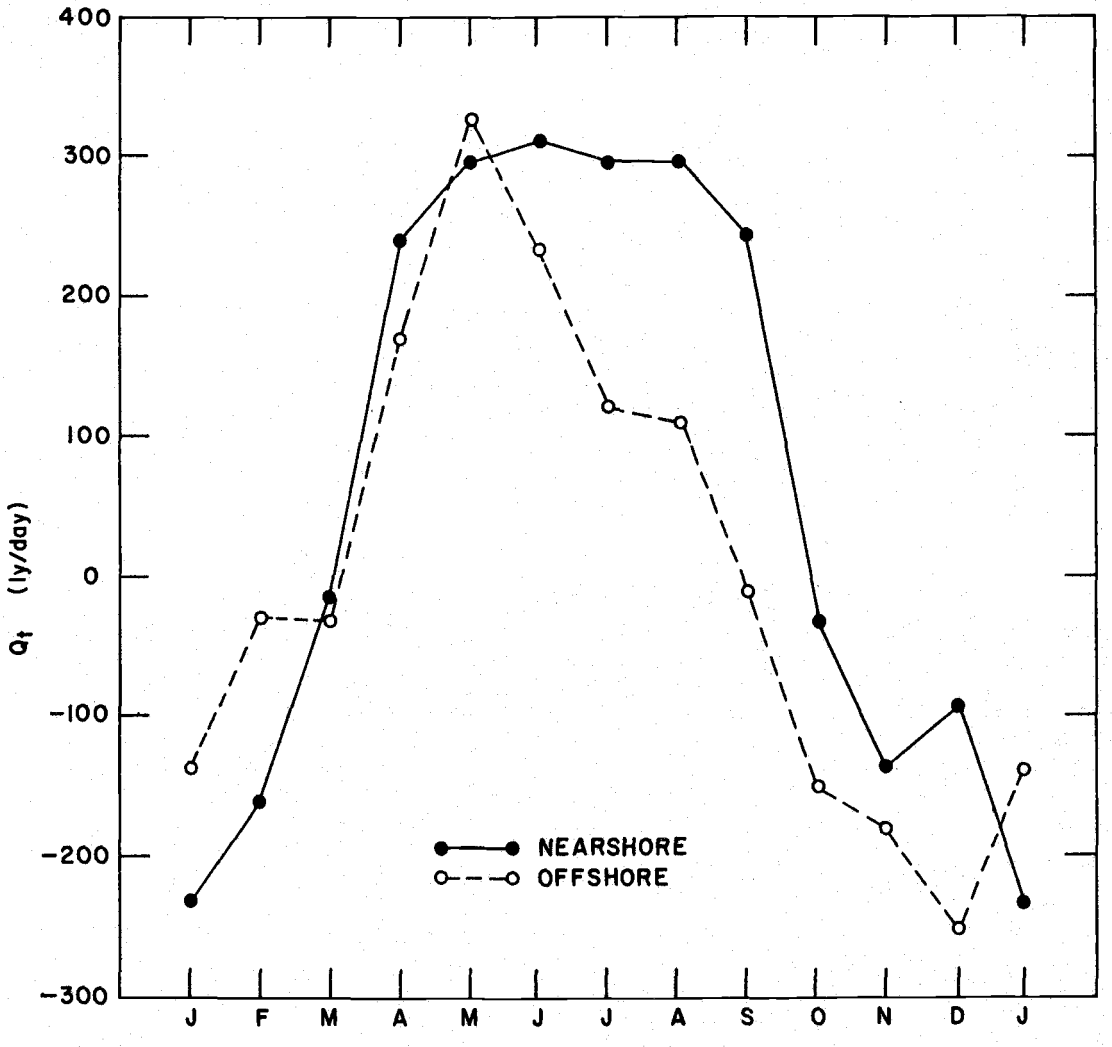

Figure 25. Comparison of nearshore and offshore region values of 10-year (1953 to 1962) means of daily totals of net heat exchange, Q_t.

decreases to become negative in September. In the nearshore region, however, T_s values decrease in September while Q_t values remain positive until October. The vertical advection of cool water (upwelling) is therefore an additional important heat budget term to be considered in the nearshore region during the late summer and autumn. It is recommended that studies of total heat content of the ocean beneath the nearshore region of the sea surface be carried out in conjunction with measurements of air-sea heat exchange. As this thesis is written, the author is pleased to note that preparations for such a study, using radiation measuring devices for the attainment of precise heat exchange values, and bathythermograph data for determinations of total heat content, are being made.

UPWELLING AND THE CLIMATE OF OREGON

Upwelling and the Oceanic Climate: A Summary

Preparatory to an examination of the effects of upwelling on the climate of the coastal region of Oregon, it is necessary to summarize the effects of this process on the climate of the airmass overlying the nearshore waters off the coast of Oregon. If it could be assumed that the air mass trajectory was always from the offshore direction, upwelling was the only oceanic process altering air-sea exchanges, and there were no atmospheric or oceanographic gradients superimposed over or in the coastal system, a direct comparison of offshore and nearshore data could be made to determine the effects of upwelling.

The trajectory of low level air masses in the region of study may be taken to correspond to the surface wind direction. Charts 3, 15, 23, 31, 43, 51, 59, 71, 79, 87, 99, and 107 of the Climatological and Oceanographic Atlas for Mariners (39) contain "wind-roses" at the position 41°00' N and 126°00' W. These long-term averages of wind direction frequency are summarized in Table VIII. The airflow near the coast of Oregon is directed predominantly onshore or alongshore. Offshore winds are most frequent during winter months (beginning to increase in frequency in September) and by December reach only 20 percent of the total wind directions recorded or about half of

each of the onshore and alongshore components. Thus, the effects of passage over land in the analyses of summer climatic changes in the coastal region may be ignored.

Table VIII. Long-term monthly means of wind direction frequency at 41°00' N, 126°00' W (39).

Directed	Jan	Feb	Mar	Apr	May	Jun	Jul	Aug	Sep	Oct	Nov	Dec
						Percent						
Onshore	40	44	48	55	53	54	40	48	39	44	47	39
Along-shore	34	35	34	29	28	34	47	39	44	38	29	37
Offshore	18	12	11	7	11	4	5	5	9	10	13	20

It has been pointed out that the Columbia River effluent may be responsible for containing heat near the surface of the offshore region and thereby promoting higher than normal surface water temperatures. To effectively study the long-term effects of the above, a general oceanographic survey lasting several years, of the entire Overall Region, would be required. The occurrence of this water will follow the peak runoff from the river, which normally occurs from May to July (41), and it will most effectively influence surface temperature gradients when it occurs in dilute pools along the coast (11). Since this phenomenon has an effect on the climate opposite to that of the upwelling process, since it occurs during the upwelling season, and since it is virtually impossible to numerically determine its relative effect from the data available for the years being studied, it must

be considered merely as a normal feature of the offshore region.

The initial air and sea surface temperature gradients (which the atmospheric and oceanic systems had before entering the upwelling region) were subtracted from the gradients between the offshore and nearshore sub-regions. The initial gradients were determined for use in a previous section (Table II). Also, monthly values of the differences between the original gradients and the observed gradients for the years studied are contained in Table II. The net effect of coastal processes on the sea surface temperatures ((2)-(1), in Table II), clearly indicates a peak effect in early autumn of reduced nearshore temperatures. This effect carries through until January, when the effect is reversed. The plus values indicate a late winter and early spring nearshore warming (i. e. lack of cooling) brought about by coastal processes (convergence).

Values of the net effect of coastal processes on the air temperature gradients normal to the coast are indicated in Table II, row (4)-(3). The pattern is similar to the effects on sea temperature but is complicated by the possibilities of winter offshore air flow. In summer and early autumn, however, it is clear that coastal processes have a net effect of cooling the nearshore surface air mass.

The summarized differences in air temperature, T_a; relative humidity, R. H.; heat lost to the atmosphere, Q_l (where $Q_l = Q_e + Q_h + Q_b$); moisture lost to the atmosphere, E; and cloud cover, c between

the sub-regions are listed in Table IX.

In Table IX it is seen that if an air mass trajectory from sea to land is assumed, the upwelling process results in the air temperature being lower by 3 F^{o} in the nearshore region than the offshore region, the nearshore relative humidity a few meters above sea level is higher than offshore, and evaporation is lower in the nearshore region than it is offshore. These conclusions rely upon assuming that relative humidity and evaporation would change but slightly from offshore to nearshore in the absence of upwelling. Despite the lower values of evaporation in the nearshore region during this upwelling period,

Table IX. Mean monthly differences between nearshore and offshore sub-regions of: air temperature (T_a in ^{o}F), relative humidity (R. H. in percent), heat loss to the atmosphere (Q_1 in langleys per day), moisture loss to the atmosphere (E in inches per day), and cloud cover (c in tenths) averaged from the data used in this study.

	T_a	R. H.	Q_1	E	c
Jan	2.9	-4.4	122	0.06	-1.9
Feb	-1.2	-7.1	95	0.06	1.2
Mar	0.7	2.0	-31	-0.01	0.4
Apr	1.8	-1.1	-47	-0.02	-0.3
May	0.8	0.4	26	0.03	0.2
Jun	-1.4	-1.0	-47	-0.03	-0.5
Jul	-1.1	7.5	-186	-0.10	0.2
Aug	-3.1	3.0	-99	-0.05	-1.5
Sep	-2.4	4.1	-217	-0.10	-0.8
Oct	-0.4	2.0	-89	-0.06	-1.1
Nov	1.0	0.5	-47	-0.04	0.1
Dec	4.0	9.2	-134	-0.08	-2.0

cooling results in higher relative humidities and one expects a higher frequency of fog near the coast. The actual smaller amount of cloud cover in the nearshore region must be attributed to a smaller amount of middle and high cloud near the continent.

In winter months, convergence in the nearshore region results in higher air temperature, lower relative humidity, and a slight increase in evaporation here than in the offshore region.

Upwelling and the Climate of Coastal Oregon

It has been shown that both winter and summer oceanic processes influence the climate in the nearshore region off Oregon. In order to demonstrate the influence of upwelling on the climate of the coastal region of Oregon, data from several U.S. Weather Bureau stations along the coast were chosen for analysis. As mentioned previously, upwelling will be weaker in regions where there is a strong river effluent imposed on the coastal system. The Astoria station (Fig. 1) was chosen as a station whose climate is less strongly influenced by upwelling since it is situated at the mouth of the Columbia River.

Comparisons of mean monthly values of T_a for Astoria, Newport, and Brookings, Oregon (Fig. 1) are contained in Figure 26. The two more southerly stations maintain a temperature difference of

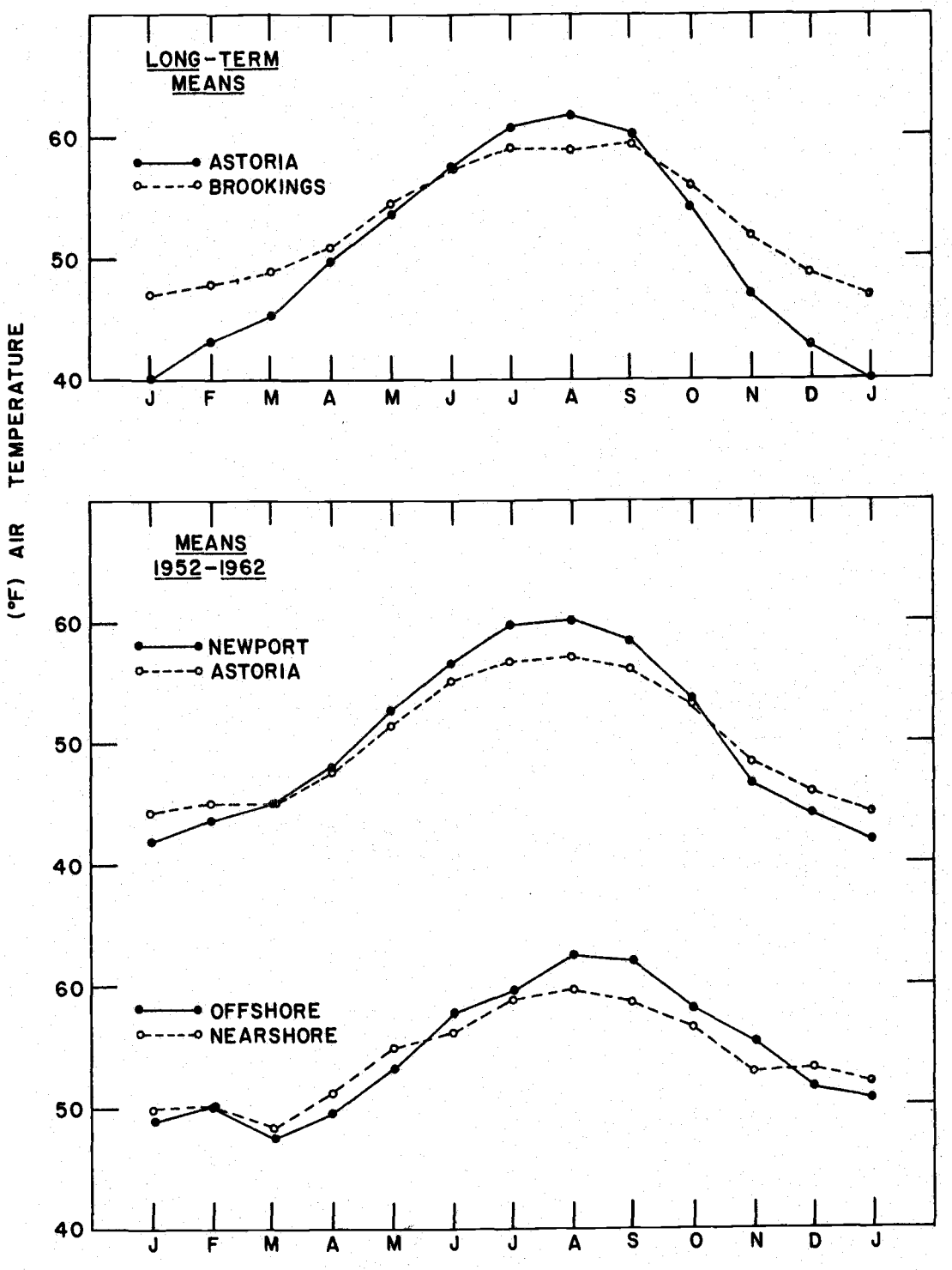

Figure 26. Comparison of mean values of air temperature between Astoria and Brookings, Astoria and Newport, and the nearshore and offshore sub-regions. (See Fig. 1 for all positions)

about 3 F^{o} throughout the year; the most southerly station (Brookings) being warmer. The values of T_a at Astoria, however, rise above those at both the other stations during July and August. Allowing the differences between the Brookings and Newport values to be due to latitudinal variations and extrapolating to the Astoria latitude, it is found that the projected values of T_a are from 0.5 to 1.5 F^{o} too low in winter and almost 6.0 F^{o} too low in summer. In order to attribute this to summer upwelling, it must be assumed that the airflow is always from the sea. The long term monthly means of wind direction for Astoria (Table III) show that there is a mean westerly component at Astoria only from April to August, inclusive. By confining conclusions to this period, it may be said that the data reveals a definite influence of upwelling (note the comparison of nearshore and offshore T_a values also included in Figure 26) on the air temperatures of the coastal areas of Oregon.

Except for the station at Astoria, the U.S. Weather Bureau station at North Bend, Oregon (Fig. 1) is the only one for which the Weather Bureau publishes monthly means of relative humidity. Thirty-year means of this data from North Bend for the times 4:30 a.m. and 4:30 p.m. (Pacific Standard time) are plotted in Figure 27 with thirty-year means from Astoria for the times 4:00 a.m. and 4:00 p.m. Again, as with the Astoria station, the records reveal

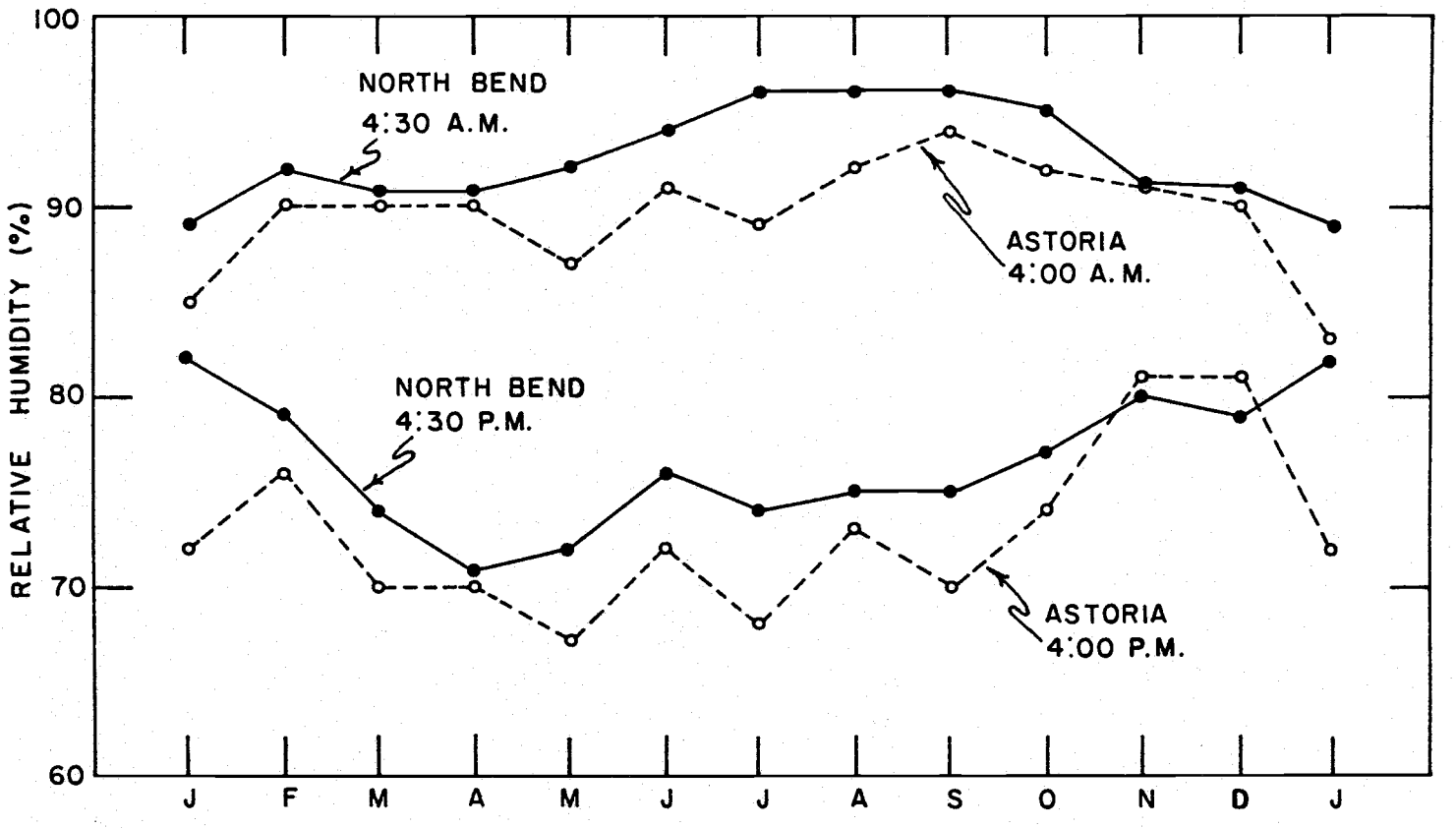

Figure 27. Comparison of mean relative humidity values at Astoria and North Bend for morning and afternoon periods. (See Fig. 1 for all positions)

that only in the summer months is North Bend, on the average, subject to winds with a westerly component. Limiting the discussion to these months, it is seen in the data of relative humidity that the average summer value (May to August) at Astoria is about 4.5 percent lower than that at North Bend. This corresponds closely to the difference between the relative humidity values of the two sub-regions. The data, therefore, support the contention that the nearshore oceanic processes affect the relative humidities in the coastal region of Oregon by raising their values.

SUMMARY OF OBSERVATIONS AND CONCLUSIONS

This is the first study of its kind in the region adjacent to the Northwest United States. There is, therefore, a large number of items described in the results of the study which may be considered as legitimate products of the study and contributions to the findings of the research. However, several items have been brought to light which must be considered as being of greater basic interest either because of their fundamental contribution to the understanding of oceanographic-meteorological processes in this region or because of their being contrary to expectation. These results are now summarized.

1. In the Overall Region, maximum sea surface temperatures frequently occur in September, about one month later than maximum air temperatures. Winter minima of T_s also frequently occur later than minima of T_a.

2. The highest values and largest range of monthly wind speed averages in the Overall Region occur in winter.

3. Cloud cover varies considerably from month to month but shows no definite seasonal variation.

4. Winter values of T_s are higher than those of T_a in the Overall Region. This is also the case along Vancouver Island, but not at Station P and thus appears to be a coastal phenomenon,

resulting from nearshore convergence.

5. The climatological data from the sub-regions clearly show the effects of summer upwelling. Upwelling results in a lowering of air, sea, and wet bulb temperatures in the nearshore region. The vapor pressure difference, $e_s - e_a$ (important to vertical mass transfer), is greatly reduced in the nearshore region.

6. Offshore transports in summer, due to upwelling, may be smaller in magnitude than onshore transports in winter. However, the summer upwelling process is more influential than winter convergence in altering surface temperature distributions near the coast because horizontal and vertical temperature gradients are larger in the summer months. Therefore, there is a net annual lowering of sea surface temperatures along the Oregon coast. There is little net annual alteration of air temperatures or temperature gradients due to the convergence or divergence processes along the Oregon coast.

7. Although upwelling is most dramatically a summer and autumn feature, northerly winds in winter months can also result in upwelling or at least in a relaxation of convergence.

8. Sea surface temperatures in the region just seaward of the upwelling zone frequently are higher in value than air temperatures in this region. A suggested reason for this is that the effluent of the Columbia River produces a vertical stability in the upper part of the

ocean which conserves heat near the surface. There is no evidence that this process significantly affects the climate of coastal Oregon.

9. The total heat budget for the Overall Region features a strong heat input to the sea in summer and a weak net input or output in winter. The net heat exchange varies considerably from year to year and, in one of the years studied, an annual net heat loss from the sea was computed. Generally, however, the sea adjacent to the Pacific Northwest receives a net annual input of heat from air-sea exchange.

10. Heat loss due to evaporation at the sea surface accounts for about twice the heat lost due to net back radiation. Latent heat loss is generally greater than four times the heat loss due to reflection of long wave radiation at the sea surface or heat conducted away from the sea in the Overall Region.

11. The factors which most determine the differences in the heat budget from year to year are variations in cloud cover, sea surface temperature, and wind speed.

12. Monthly values of net heat exchange, Q_t, may be roughly estimated from predicted "pan" evaporation (E') and computed "real" evaporation (E) by:

$$Q_{net} = f(E' - E)$$

13. Upwelling in summer affects the heat budget by slightly reducing the back radiation, greatly reducing conduction from the sea to the atmosphere (conduction to the sea may occur frequently in the upwelling season), and greatly reducing the heat loss due to evaporation. Because of the relative magnitudes involved, the latter is the most important effect. Suppression of nearshore evaporation by upwelling results in the reduction of water transfer to the atmosphere by about 2 inches a month in the summer and early winter months.

14. Total heat budget analyses of the surface water in the nearshore region should include a term for vertical advection. Because of strong vertical temperature gradients in the summer, this term is probably more important than one for horizontal heat advection parallel to the coast. The vertical advection of heat in the nearshore region will be similar in magnitude to the horizontal advection of heat from the nearshore region to the offshore region.

15. The measurable effects of upwelling on the climate of coastal Oregon are a suppression of the summer and autumn-air temperature values and an increase in relative humidity.

BIBLIOGRAPHY

1. Anderson, E. R., L. J. Anderson and J. J. Marciano. A review of evaporation theory and development of instrumentation. San Diego, 1950. 70 p. (U. S. Navy Electronics Laboratory. Report 159)

2. Black, J.N. The distribution of solar radiation over the earth's surface. Archiv fur Meteorologie, Geophysik und Bioklimatologie, Ser. B., 10:182-192. 1960.

3. Blanton, J. O. Energy dissipation in a tidal estuary. Master's thesis. Corvallis, Oregon State University, 1964. 80 numb. leaves.

4. Bowen, I. S. The ratio of heat losses by conduction and by evaporation from any water surface. Physical Review, Ser. 2, 27: 779-787. 1926.

5. Bruce, J. P. and G. K. Rodgers. Water balance of the Great Lakes. Toronto, 1962. 29 p. (Great Lakes Institute, GLI 7)

6. Budyko, M. I. The heat balance of the earth's surface. Washington, U. S. Department of Commerce, 1954. 259 p. (Office of Technical Services translation PB 131692)

7. Burt, W. V. Albedo over wind-roughened water. Journal of Meteorology 11(4):283-290. 1954.

8. Burt, W. V. Heat budget terms for Middle Snake River reservoirs. Corvallis, 1958. 23 p. (Oregon State University Technical Report 6)

9. Collins, Curtis. Structure and kinematics of the permanent oceanic front off the Oregon coast. Master's thesis. Corvallis, Oregon State University, 1964. 53 numb. leaves.

10. Defant, A. Physical oceanography. Vol. I. New York, Pergamon, 1961. 729 p.

11. Denner, W. W. Sea water temperature and salinity characteristics observed at Oregon coastal stations in 1961. Master's thesis. Corvallis, Oregon State University, 1962. 72 numb. leaves.

12. Fritz, S. Solar radiant energy and its modification by the earth and its atmosphere. In: Compendium of meteorology, ed. by T. F. Malone. Boston, American Meteorological Society, 1951. p. 13-33.

13. Haltner, G. J. and F. L. Martin. Dynamical and physical meteorology. New York, McGraw-Hill, 1957. 470 p.

14. Haurwitz, B. and J. M. Austin. Climatology. New York, McGraw-Hill, 1944. 410 p.

15. Jacobs, W. C. The energy exchange between sea and atmosphere and some of its consequences. Bulletin of the Scripps Institute of Oceanography 6(2):27-122. 1951.

16. Kimball, H. H. Amount of solar radiation that reaches the surface of the earth on the land and on the sea, and methods by which it is measured. Monthly Weather Review 56(10):393-398. 1928.

17. Lane, R. K. A review of the temperature and salinity structures in the approaches to Vancouver Island, British Columbia. Journal of the Fisheries Research Board of Canada 19(1):45-91. 1962.

18. Lane, R. K. Estimating evaporation from insolation. Hydraulics Journal, American Society of Civil Engineers 90(HY5):33-41. 1964.

19. Lane, R. K. Wind, nearshore ocean temperatures, and the tuna catch off Oregon. Research Briefs, Fish Commission of Oregon (in press).

20. Laevastu, T. Factors affecting the temperature of the surface layer of the sea. Societas Scientiarum Fennica, Commentationes Physico-Mathematicae 25(1):1-135. 1960.

21. Leipper, D. F. Fog development at San Diego, California. Journal of Marine Research 7(3):337-346. 1948.

22. Lonnquist, O. Synthetic formulae for estimating effective radiation to a cloudless sky and their usefulness in comparing various estimation procedures. Archiv foer Geofysik 2(12):247-294. 1954.

23. Malkus, J. S. Large-scale interactions. In: The sea, vol. 1. New York, Interscience, 1963. p. 88-294.

24. McAlister, W. B. Rogue River Basin study, Part I. Corvallis, Water Research Associates. 1961. 34 p.

25. Oregon State University. Department of Oceanography. Unpublished hydrographic data. Corvallis, 1959 and 1960.

26. Oregon State University. Department of Oceanography, Corvallis, 1962. 77 p. (Data Report No. 7 (62-6))

27. Penman, H. L. Estimating evaporation. Transactions of the American Geophysical Union 37(1):43-50. 1956.

28. Pickard, G. L. and D. C. McLeod. Seasonal variation of the temperature and salinity of surface waters of the British Columbia coast. Journal of the Fisheries Research Board of Canada 10:125-145. 1953.

29. Smithsonian Institution. Smithsonian meteorological tables. 6th ed. Washington, 1951. 527 p.

30. Spilhaus, A. F. A bathythermograph. Journal of Marine Research 1:95-100. 1938.

31. Stephans, J. C. and E. H. Stewart. A comparison of procedures for computing evaporation and evapotranspiration. International Association of Scientific Hydrology Publication 62:123-142. 1963.

32. Sverdrup, H. U. On the process of upwelling. Journal of Marine Research 1(1):155-164. 1938.

33. Sverdrup, H. U. Oceanography for meteorologists. New York, Prentice Hall, 1943. 246 p.

34. Sverdrup, H. U. Evaporation from the oceans. In: Compendium of meteorology, ed. by T. F. Malone. Boston, American Meteorological Society. 1951. p. 1071-1081.

35. Sverdrup, H. U., M. W. Johnson, and R. H. Fleming. The oceans. Englewood Cliffs, Prentice-Hall, 1942. 1087 p.

36. Tabata, S. Temporal changes of salinity, temperature, and dissolved oxygen content of the water at Station "P" in the northeast Pacific Ocean, and some of their determining factors. Journal of the Fisheries Research Board of Canada 18(6):1073-1124. 1961.

37. Tully, J. P., A. J. Dodimead, and S. Tabata. An anomalous increase of temperature in the ocean off the Pacific coast of Canada through 1957 and 1958. Journal of the Fisheries Research Board of Canada 17(1):61-80. 1960.

38. Tully, J. P. and L. F. Giovando. Seasonal temperature structure in the Eastern Subarctic Pacific Ocean. In: Royal Society of Canada Special Publication 5. Toronto, University of Toronto Press, 1963. p. 10-36.

39. U. S. Department of Commerce. Climatological and oceanographic atlas for mariners, vol. II. Washington, 1961. 159 charts.

40. U. S. Department of Commerce. Climatological data, national summary, vols. 4 to 13. Asheville, 1953-1962.

41. U. S. Department of the Interior. Compilation of records of surface waters of the United States, October 1950 to September 1960: 1963. 327 p. (Geological Survey water-supply paper 1738)

42. U. S. Geological Survey. Water loss investigations: Lake Hefner studies, Technical Report. 1954. 158 p. (Professional Paper 269)

43. U. S. Geological Survey. Water loss investigations: Lake Mead studies. 1958. 100 p. (Professional Paper 298)

44. Watanabe, N. Hydrographic conditions of the North-Western Pacific. Part I. On the temperature change in the upper layer in summer. Journal of the Oceanographic Society of Japan 11(3): 111-121. 1955.

45. Webster's third international dictionary. Springfield, Merriam, 1961. 2662 p.

46. Wooster, W. S. and J. L. Reid, Jr. Eastern boundary currents. In: The sea, vol. 2. New York, Interscience, 1963. p. 253-280.

APPENDIX

APPENDIX: DEFINITIONS OF TERMS

a, b	slope and intercept of correlation equations
c	amount of sky covered by clouds, in tenths
c_p	specific heat at constant pressure
e	exponential function
e_a	vapor pressure at the height of the ship's thermometers
$(e_s)_a$	saturation vapor pressure at the air temperature
e_d	saturation vapor pressure over distilled water
e_s	saturation vapor pressure
e_w	saturation vapor pressure at the wet bulb temperature
f( )	function of the bracketed items
h	height of the clouds above sea level
k	constant in mass transfer evaporation equation
p	atmospheric pressure at sea level
r	albedo ($100\ Q_r/Q_s$)
r	correlation coefficient (in Figure 22 only)
Cl	chlorinity (‰)
E	depth of water evaporated by the sea
E'	depth of water evaporated by a shallow pan
H	humidity factor (2.0)
K	temperature in Kelvin degrees (subscripts have same meanings as with T temperatures)
L	latent heat of evaporation

Q_a solar radiation energy reaching the sea surface if there were no atmosphere

Q_b $Q_{bs} - Q_{ea}$

Q_{ba} long wave radiation energy reaching the sea surface from the atmosphere

Q_{bs} long wave radiation emitted by the sea surface

Q_c energy released to the sea by chemical processes

Q_e $Q_{es} - Q_{ea}$

Q'_e energy lost at the water surface in a shallow due to evaporation

Q_{ea} energy received by the sea by condensation on the sea surface

Q_{es} energy lost at the sea surface due to evaporation of sea water

Q_f energy conducted to the sea from the earth beneath

Q_h $Q_{hs} - Q_{ha}$

Q_{ha} energy conducted to the sea from the atmosphere

Q_{hs} energy conducted to the atmosphere from the sea

Q_k kinetic energy transmitted to the sea by winds and tides

Q_l $Q_e + Q_h + Q_b$

Q_m energy received through molecular diffusion

Q_o solar radiation energy received at the sea surface when $c = 0$

Q_p energy received by the sea from heat of precipitation

Q_r solar radiation energy reflected from the sea surface

Q_s energy of solar radiation reaching the sea surface

Q_t energy used to change the temperature of the sea

Q_v energy advected to a region by ocean currents

Q_R energy received through eddy diffusion

R Bowen's ratio (Q_h/Q_e)

R_v gas constant for water vapor (0.461 joule gram $^{-1}$ $^{o}K^{-1}$)

T_a air temperature (Fahrenheit or Centigrade) at ship thermometer height

T_s sea surface temperature (Fahrenheit or Centigrade)

T_w wet bulb temperature (Fahrenheit or Centigrade) at ship thermometer height

V wind speed at ship anemometer height

γ vertical lapse rate of air temperature

θ angle of latitude